Is there a planetary influence on solar activity?

Jose A. Abreu; J. Beer, A. Ferriz-Mas, K. G. McCracken & F. Steinhilber

Space Climate 5 Symposium, Oulu, Finland | 15 – 19 June 2013

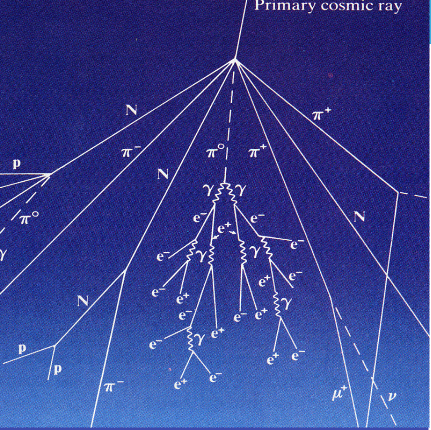

Introduction

Solar activity derived from cosmogenic radionuclides.

Solar activity and the planetary hypothesis

Some basics about solar structure

The Model

Results

Talk Summary:

Planetary influence on solar activity evidenced by cosmogenic radionulclides

- ❑ Solar activity derived from cosmogenic radionuclides
- ❑ Solar activity and the planetary hypothesis.
- ❑ Some basics about solar structure
- ❑ The model
- ❑ Results

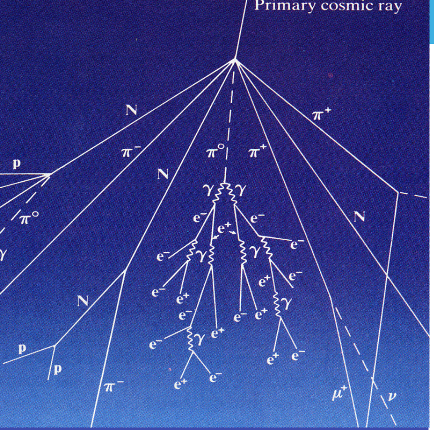

Introduction

Solar activity derived from cosmogenic radionuclides.

Solar activity and the planetary hypothesis

Some basics about solar structure

The Model

Results

Cosmogenic Radionuclides & Solar Activity

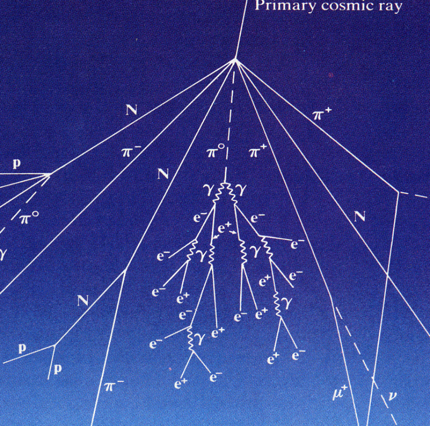

Cosmogenic radionuclides: ^{14}C and ^{10}Be

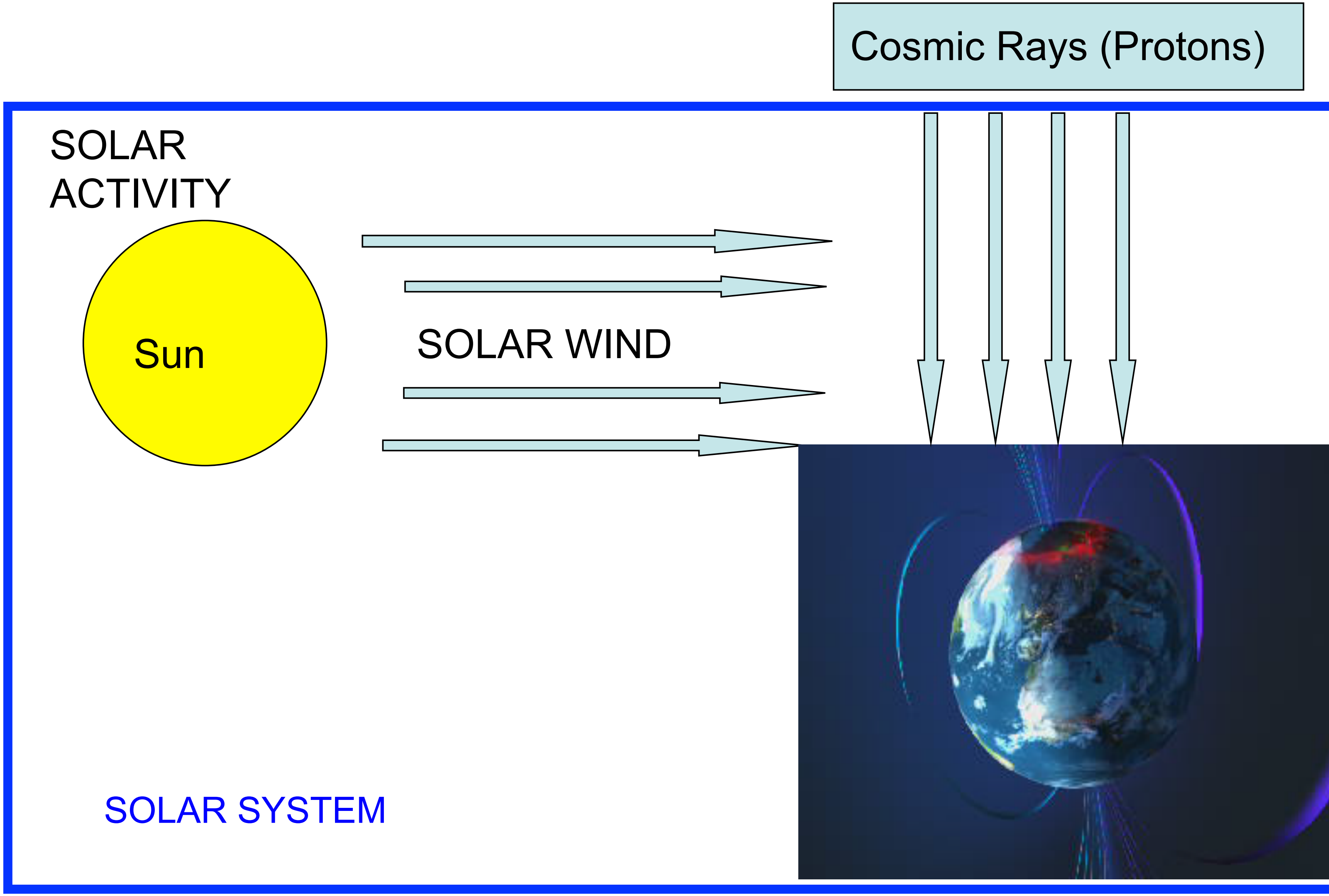

a) Solar activity for the last 10,000 years, Φ determined using ^{10}Be and ^{14}C

b) Wavelet analysis. Red high power.

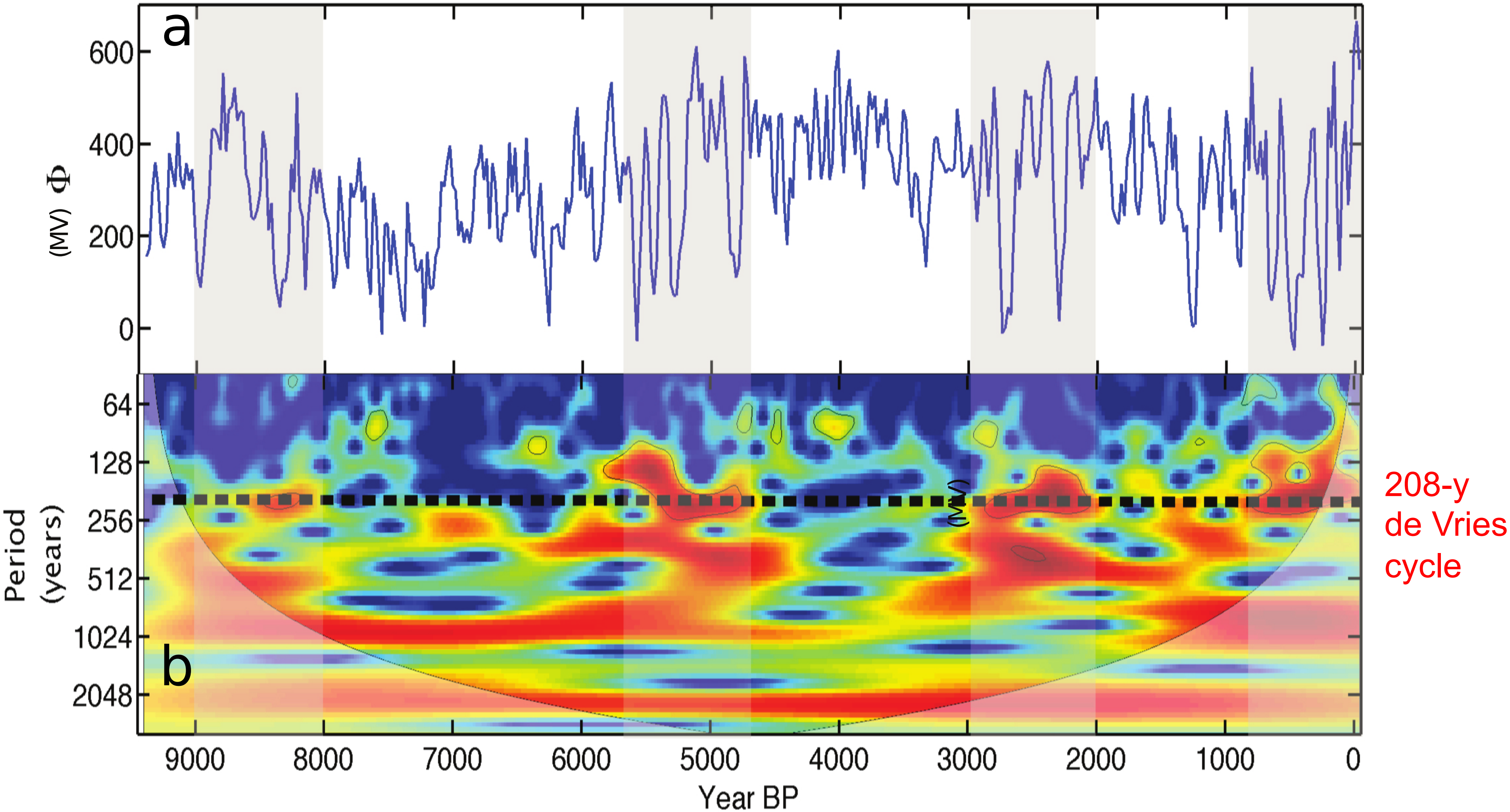

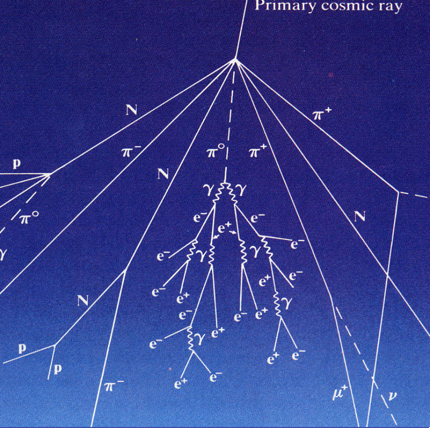

The planetary hypothesis

- Tidal acceleration is the only physically relevant interaction
- Proportional to M/d^3
- The planetary Tides on the Sun are ~ 10^{-12} surface gravity
  (for comparison on the Earth g_{moon}/g_{earth} ~ 10^{-7})
- Tide height (equilibrium tide) on the Sun does not exceed 1 mm!
- Mean daily work of tides is ~10^{28} J (Trellis, 1966)
- Comparable to the magnetic energy of the solar cycle:

$$\frac{d\phi}{dt} = 5\,10^{13}\ \mathrm{Wb/day}$$

(Galloway & Weiss 1981)

$$E_{mag} = \frac{R}{\mu}\,\phi\,B$$

(Ferriz-Mas & Steiner 2007)

For a field at the base of convection zone 1 T and 10 T => E_{mag}~10^{28} J and 10^{29} J

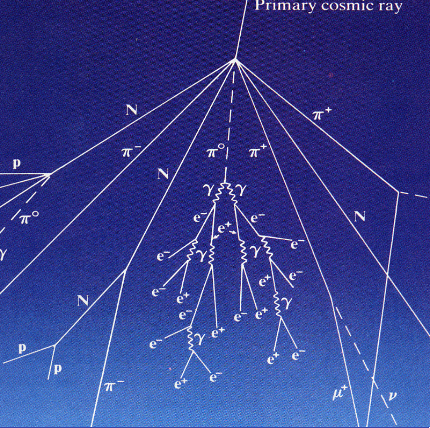

The planetary hypothesis

- Previous estimations show that the planets cannot be the cause of the 11 years solar cycle. (this would produce large changes in the orbital parameters....)
- ...however it could perturb the action of the solar dynamo.

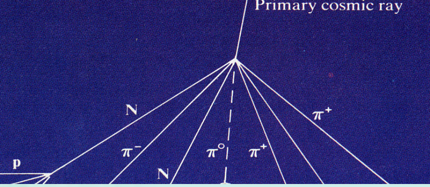

Solar Structure

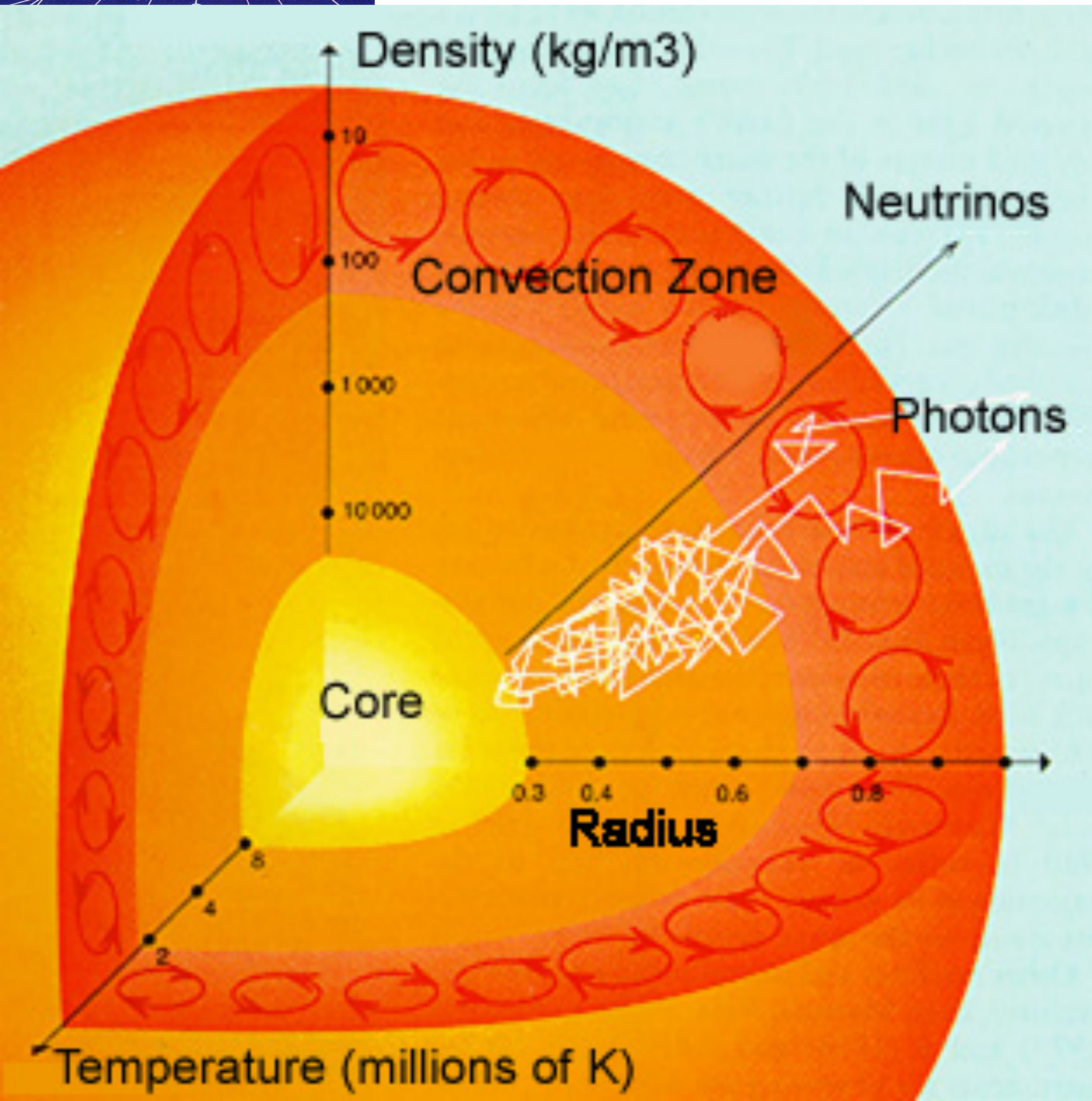

Solar Interior

1. Core
2. Radiative Interior
3. (Tachocline)
4. Convection Zone

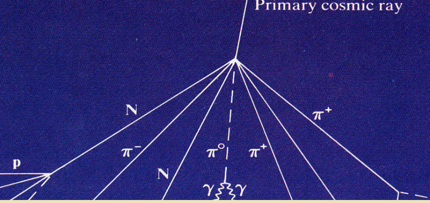

Helioseismology: Solar rotation

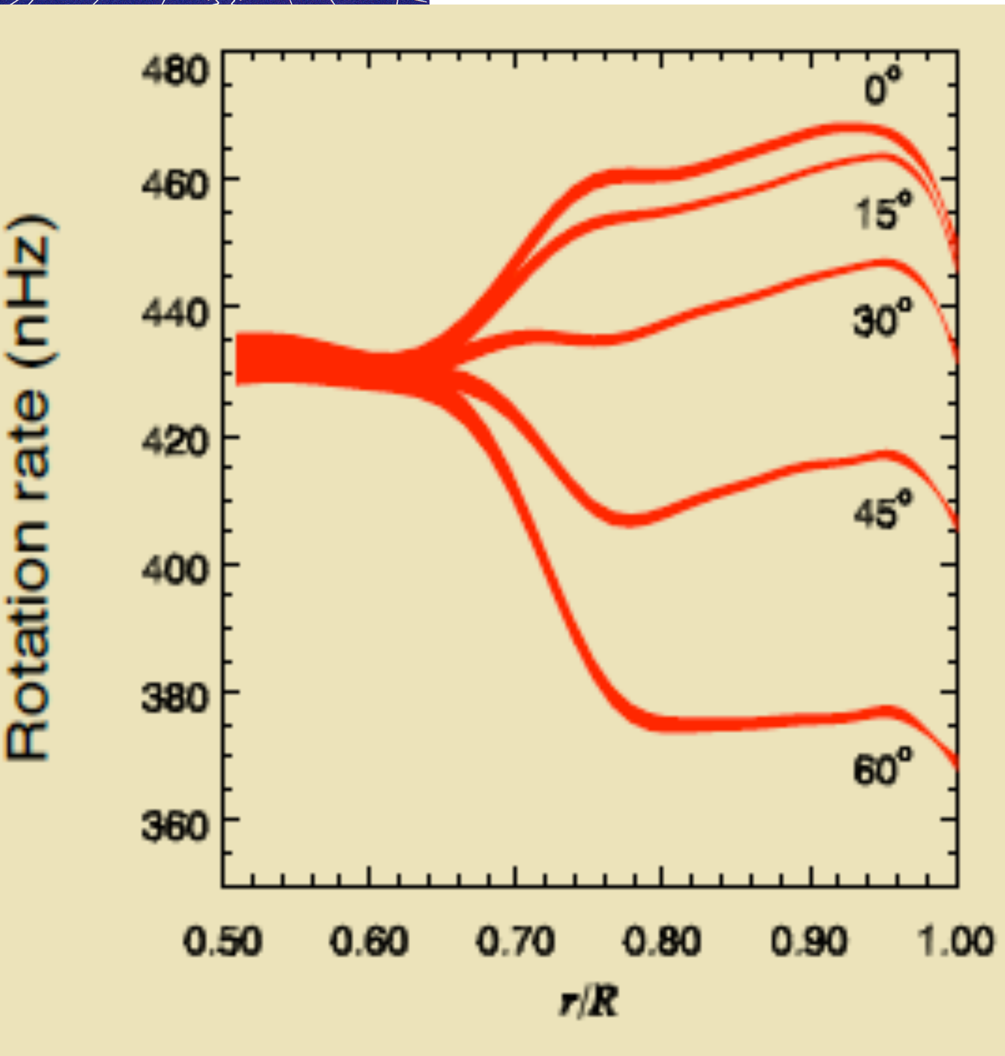

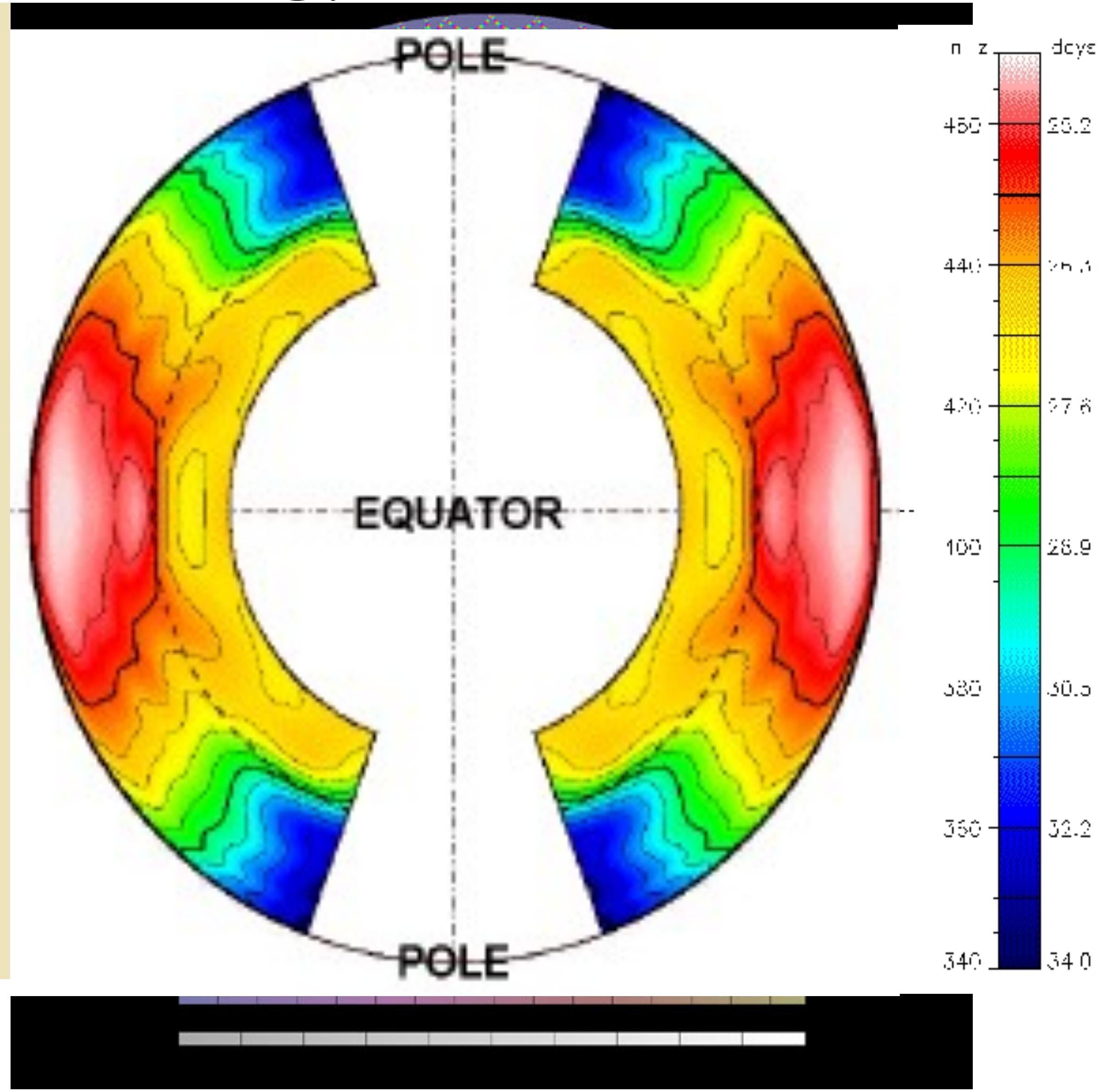

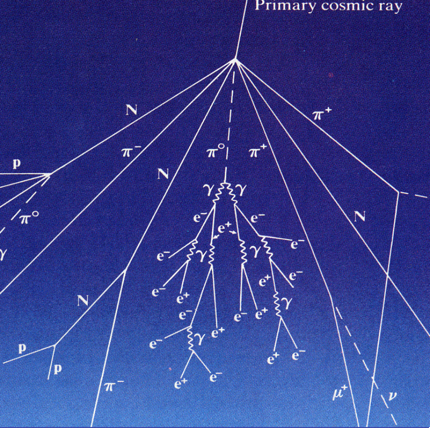

- The tachocline may play a fundamental role in the generation and storage of the toroidal magnetic flux that eventually gives rise to solar active regions
- Charbonneau et al. (1999) inferred a prolate geometry, with an ellipticity a factor 10^3 larger than the solar ellipticity at photospheric level (which is 4 times larger than the Earth's ellipticity.)

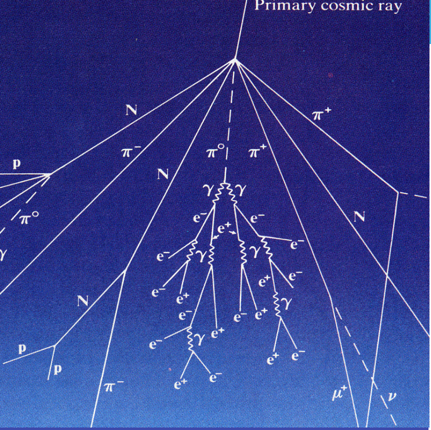

The Model

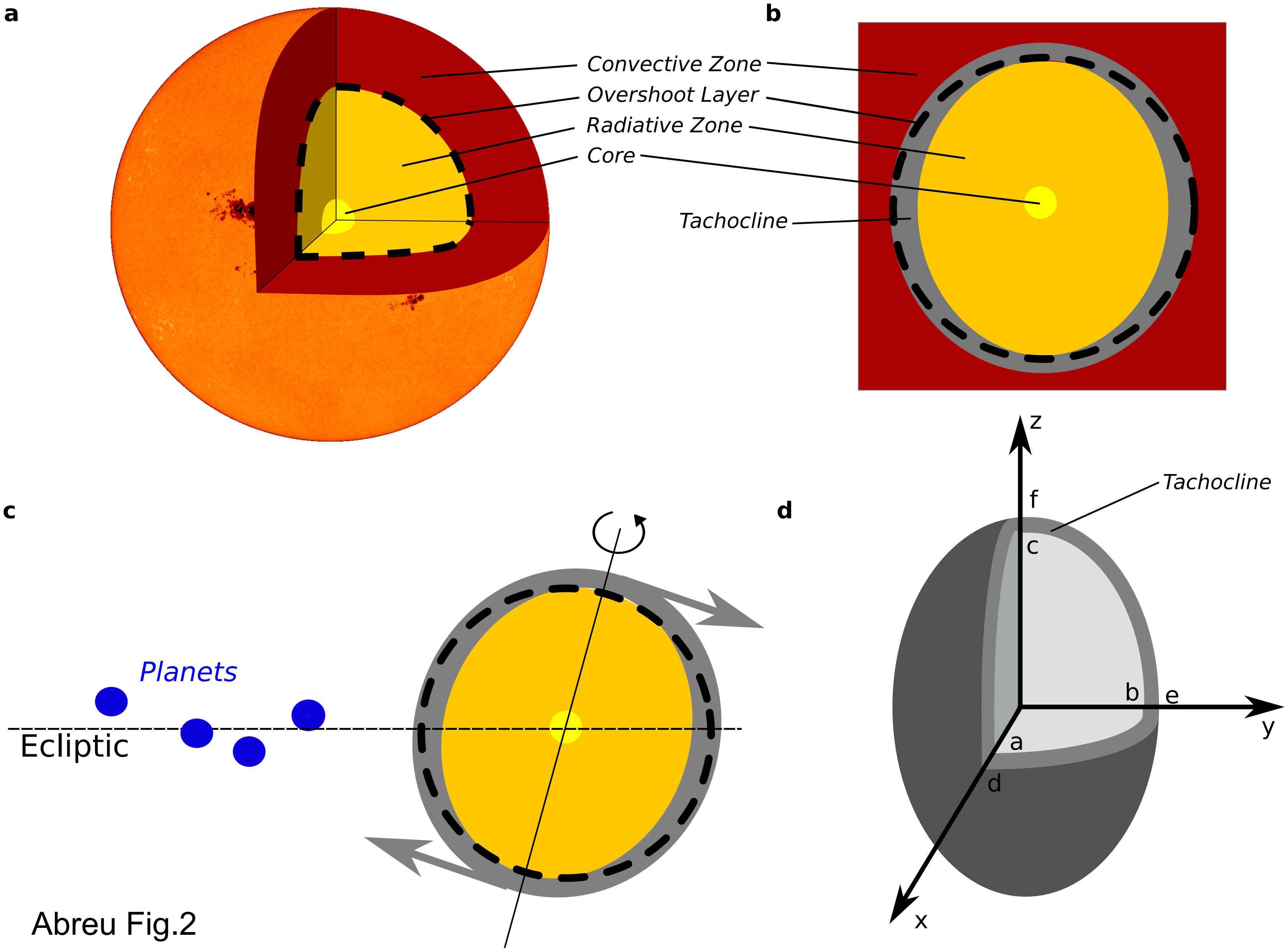

Abreu Fig.2

Introduction

Solar activity derived from cosmogenic radionuclides.

Solar activity and the planetary hypothesis

Some basics about solar structure

The Model

Results

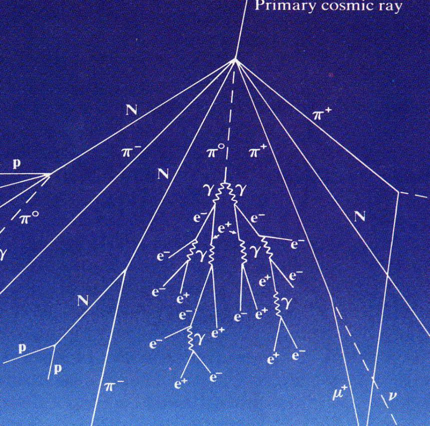

Introduction

Solar activity derived from cosmogenic radionuclides.

Solar activity and the planetary hypothesis

Some basics about solar structure

The Model

Results

The Model

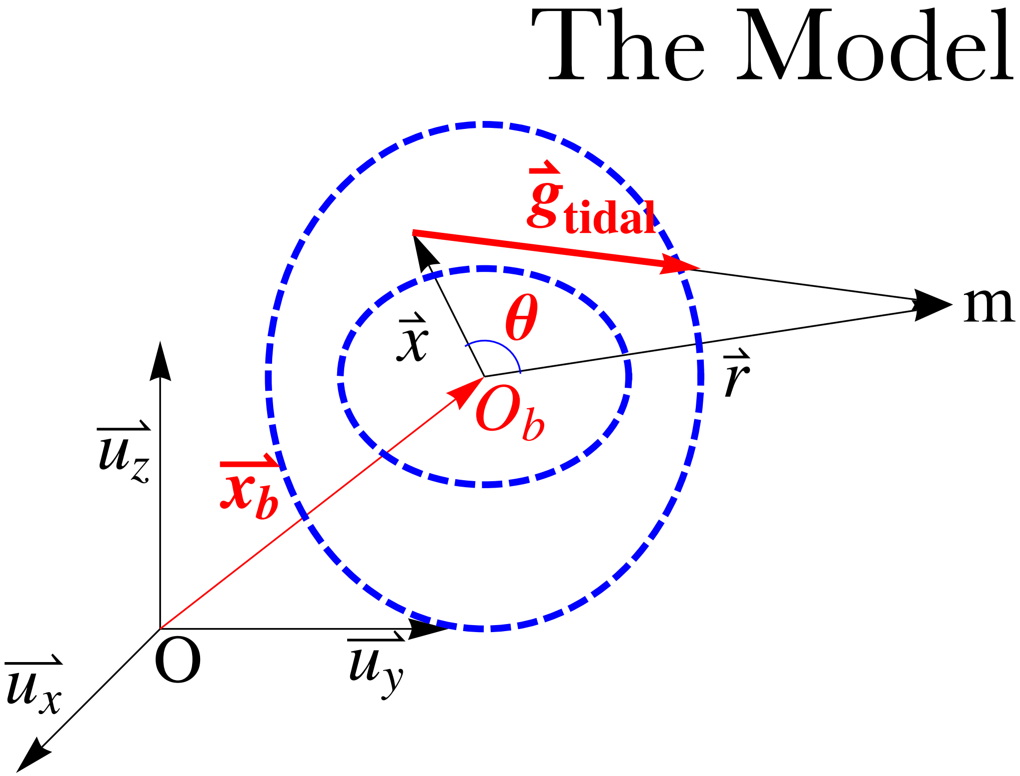

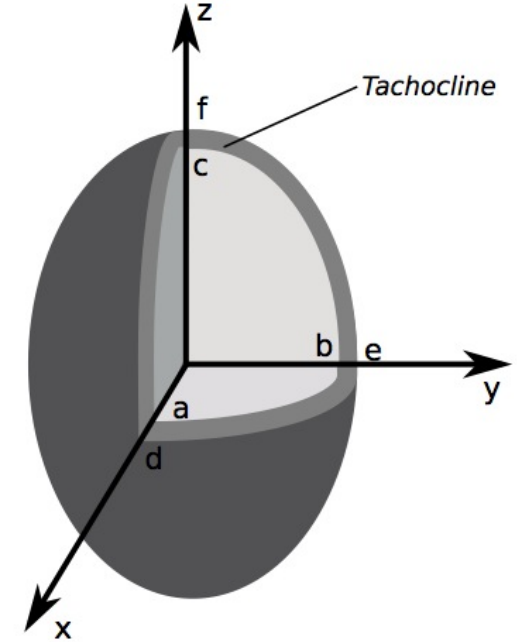

spherical geometry for the inner boundary, i.e. a=b=c

$$N_{x,i} = \mathcal{A}_i \frac{r_{y,i}\, r_{z,i}}{|\mathbf{r_i}|^5}\left[V_2(e^2 - f^2) - V_1(b^2 - c^2)\right]$$

$$N_{y,i} = \mathcal{A}_i \frac{r_{z,i}\, r_{x,i}}{|\mathbf{r_i}|^5}\left[V_2(f^2 - d^2) - V_1(c^2 - a^2)\right]$$

$$N_{z,i} = \mathcal{A}_i \frac{r_{x,i}\, r_{y,i}}{|\mathbf{r_i}|^5}\left[V_2(d^2 - e^2) - V_1(a^2 - b^2)\right]$$

where $\mathcal{A}_i = (3/5)\, G\, \rho\, m_i$, G being the gravitational constant, ρ the density of the matter in the tachocline, while $V_1 = (4/3)\,\pi a\, b\, c$ and $V_2 = (4/3)\,\pi d\, e\, f$ are the volumes of the internal and external ellipsoids, respectively

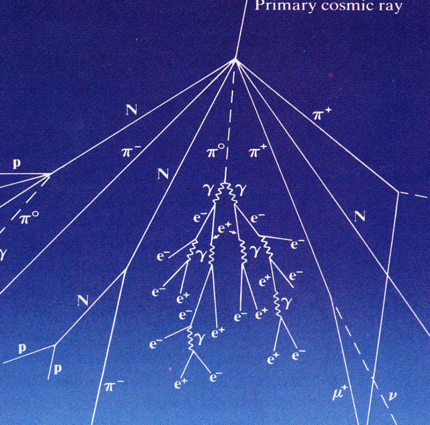

The Model

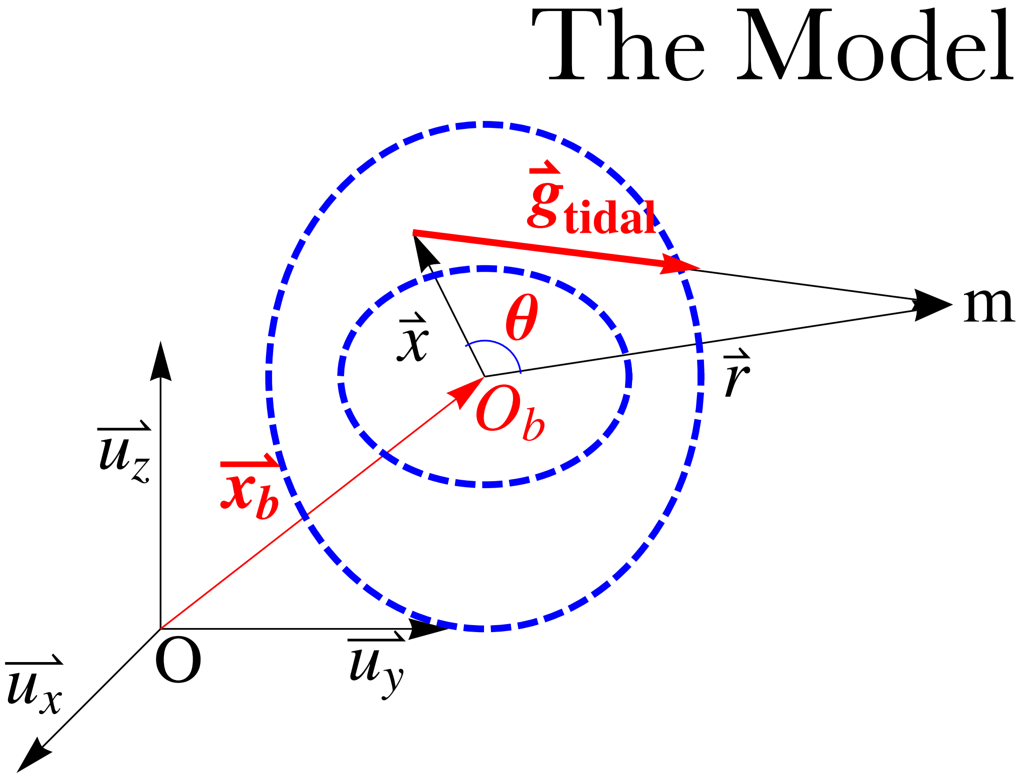

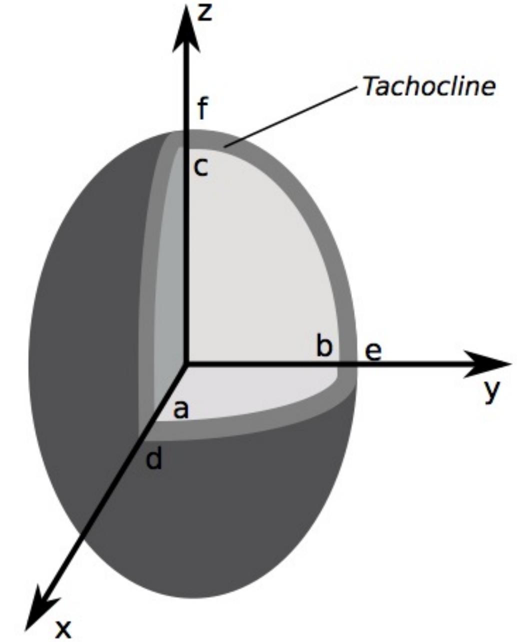

spherical geometry for the inner boundary, i.e. a=b=c

$$N_{x,i} = \mathcal{A}_i \frac{r_{y,i}\, r_{z,i}}{|\mathbf{r_i}|^5} \left[V_2(e^2 - f^2) - V_1(b^2 - c^2)\right]$$

$$N_{y,i} = \mathcal{A}_i \frac{r_{z,i}\, r_{x,i}}{|\mathbf{r_i}|^5} \left[V_2(f^2 - d^2) - V_1(c^2 - a^2)\right]$$

$$N_{z,i} = \mathcal{A}_i \frac{r_{x,i}\, r_{y,i}}{|\mathbf{r_i}|^5} \left[V_2(d^2 - e^2) - V_1(a^2 - b^2)\right]$$

3 cases:

1. e = f => N_x vanishes
2. f = d => N_y vanishes
3. d = e => N_z vanishes

where $\mathcal{A}_i = (3/5)\, G\, \rho\, m_i$, G being the gravitational constant, ρ the density of the matter in the tachocline, while $V_1 = (4/3)\,\pi a\, b\, c$ and $V_2 = (4/3)\,\pi d\, e\, f$ are the volumes of the internal and external ellipsoids, respectively

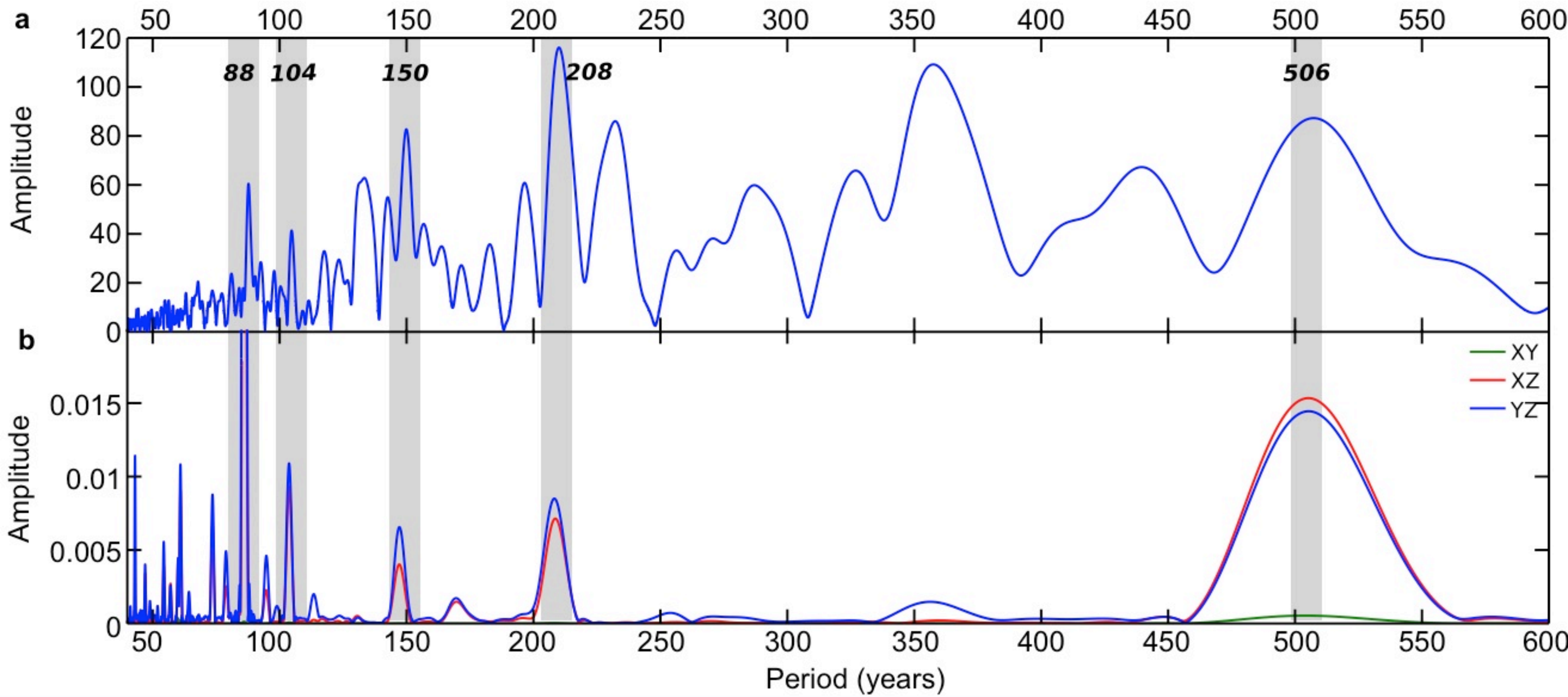

a
b
88
104
150
208
506
Amplitude
Amplitude
XY
XZ
YZ
Period (years)

case 1

b) Wavelet coherence (WTC) between Φ and torque corresponding to case 1. Red high power. The black contours shows the 5% significance regions

c) Band-pass filtered of the annually averaged torque (green curve) along with Φ (blue curve - inverted scale-) around the cycle of 208 y (de Vries)

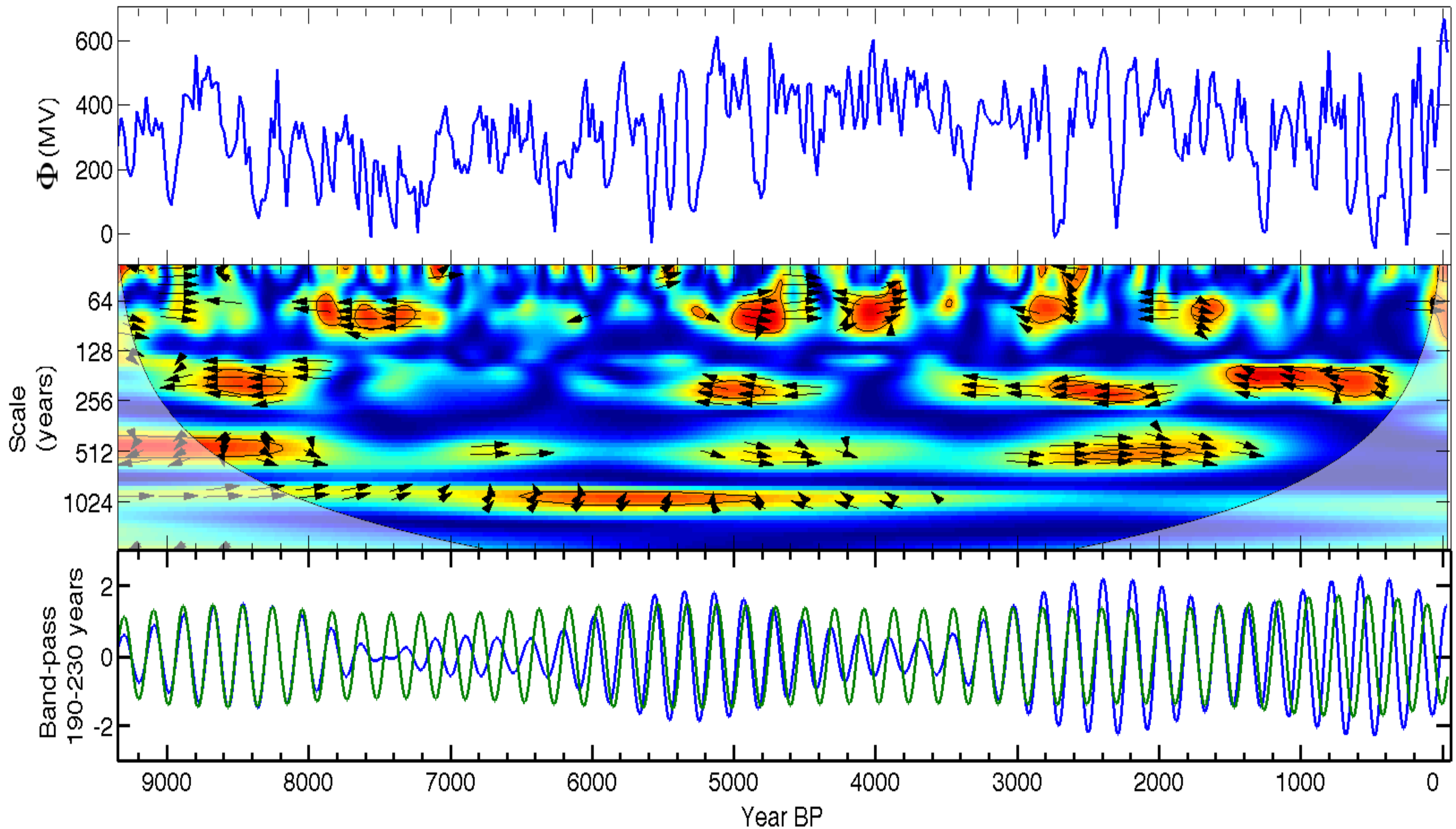

case 2

b) Wavelet coherence (WTC) between Φ and torque corresponding to case 2. Red high power. The black contours shows the 5% significance regions

c) Band-pass filtered of the annually averaged torque (green curve) along with Φ (blue curve - inverted scale-) around the cycle of 208 y (de Vries)

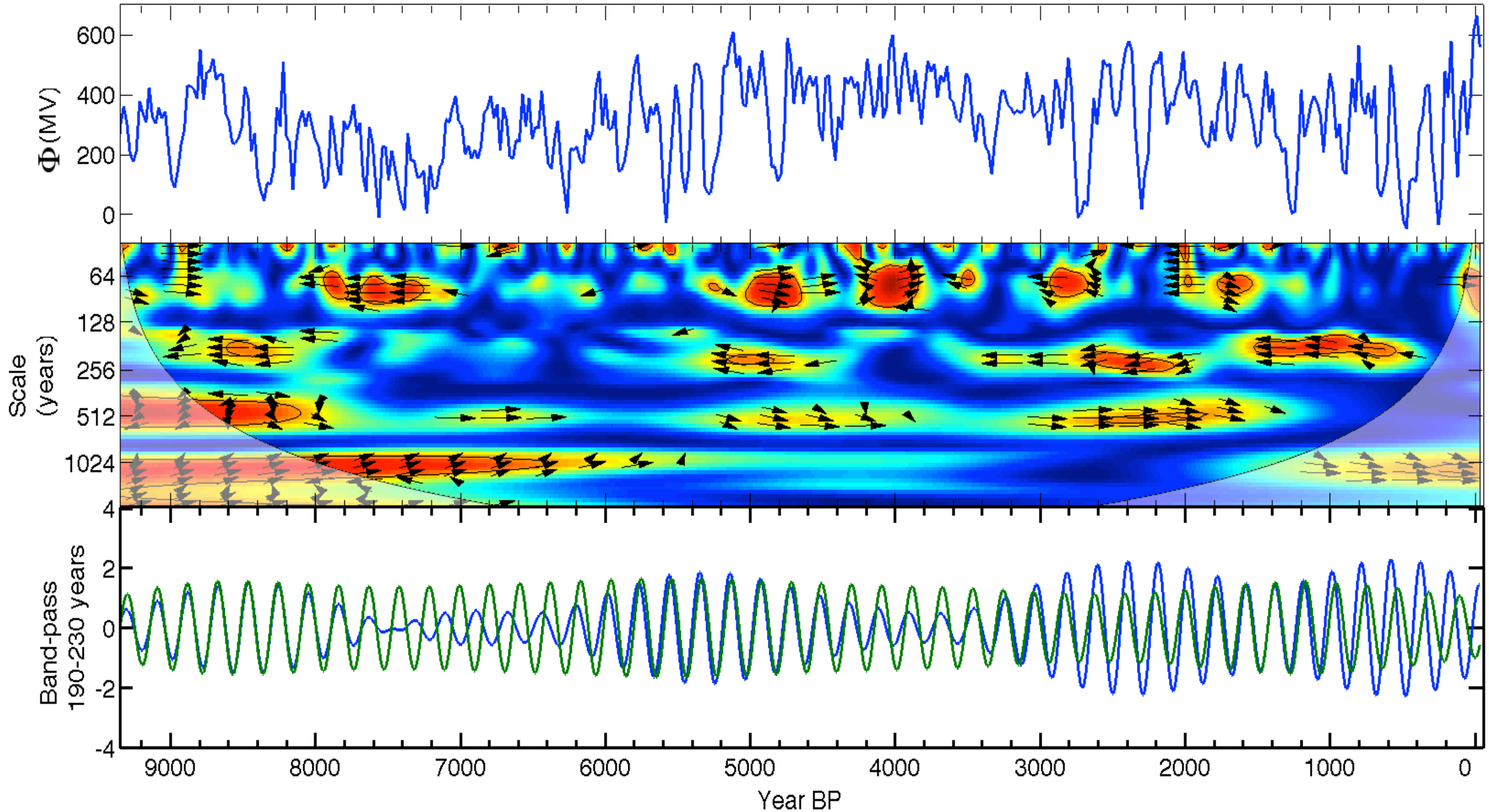

case 3

b) Wavelet coherence (WTC) between Φ and torque corresponding to case 3. Red high power. The black contours shows the 5% significance regions

c) Band-pass filtered of the annually averaged torque (green curve) along with Φ (blue curve - inverted scale-) around the cycle of 208 y (de Vries)

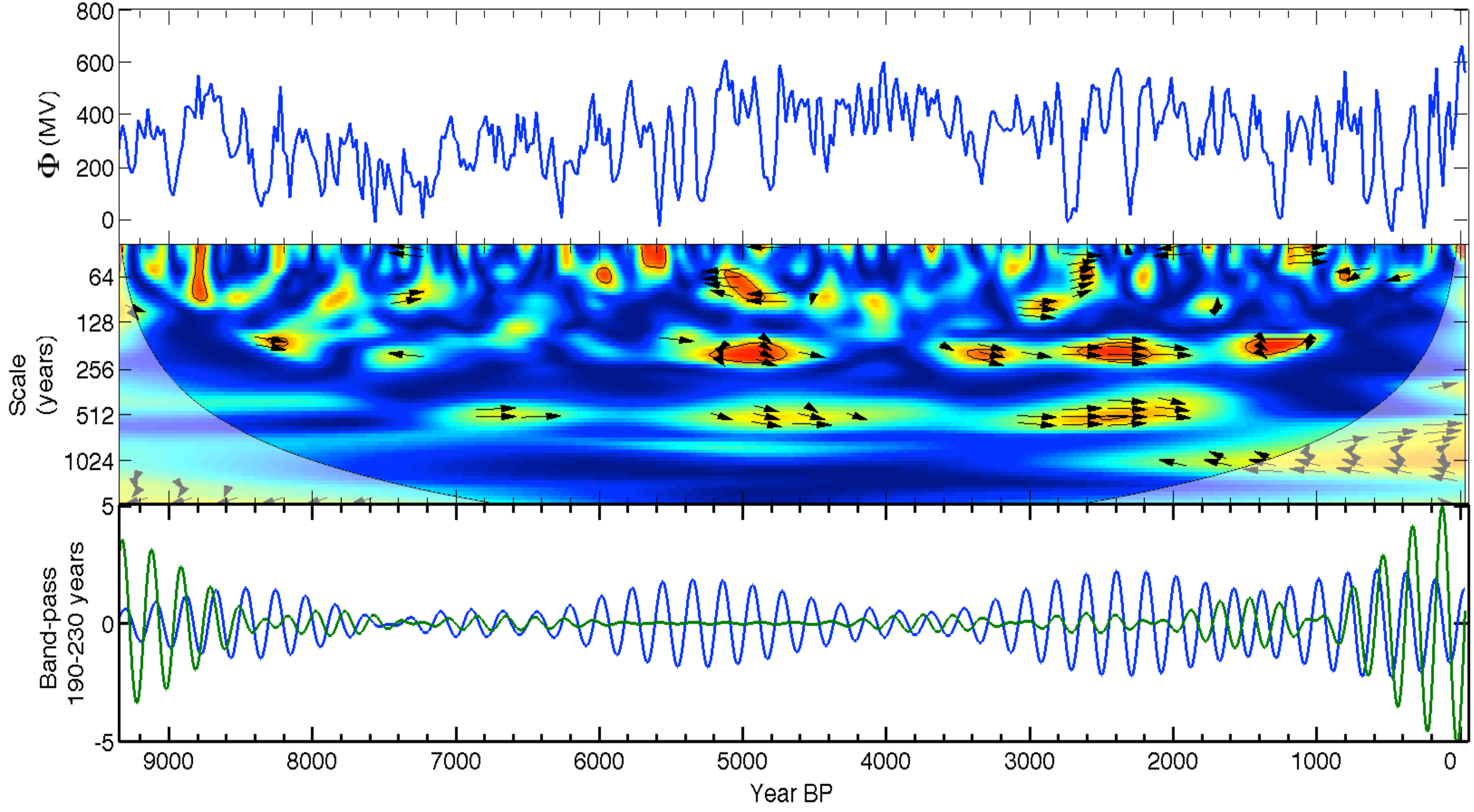

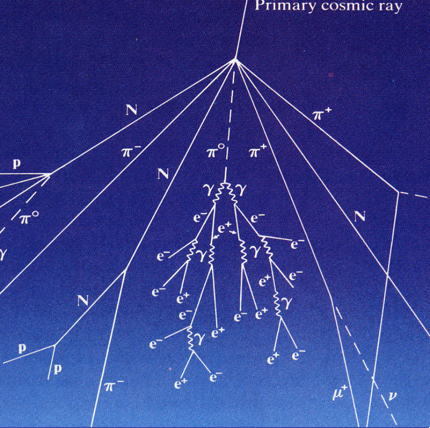

Conclusions

- The strong coherence for the 208 y band, with a constant phase of 180° (arrows pointing to the left) shows that solar activity and the planetary torque are phase locked.

- Time intervals of high coherence correspond to periods when the amplitude of the 208 y cycle is large, followed by periods of no coherence when there is no 208 y cycle, which is consistent with the clustering of Grand Minima.

- The difference between cases (1,2) and (3) points to a surprising result: a non vanishing N_z component provides the best agreement between torque and solar activity. This would imply the existence of a torque component parallel to the solar spin => the geometry of the tachocline would be a triaxial ellipsoid (either oblate or prolate).

- Our results point to a modulation of solar activity by the planets.

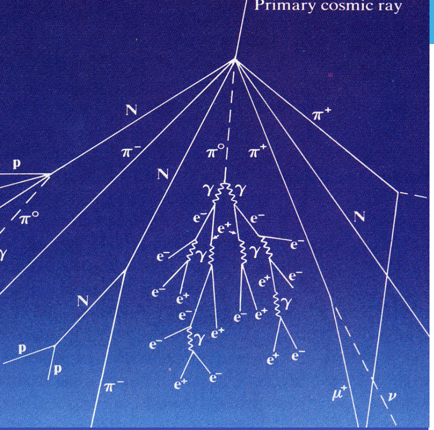

Thanks!

J. Fluid Mech. (1968), *vol.* 34, *part* 3, *pp.* 531–549
Printed in Great Britain

Resonant gravity-wave interactions in a shear flow

By ALEX. D. D. CRAIK
Department of Applied Mathematics, University of St Andrews, Fife, Scotland

(Received 22 March 1968)

Among a triad of gravity waves in a uniform shear flow, a remarkably powerful second-order resonant interaction may take place. This interaction is characterized by large growth rates of waves which propagate in directions oblique to that of the primary flow, and by a systematic transfer of energy from the primary flow to such waves. Most of the energy transfer takes place in the vicinity of a 'critical layer', where viscous forces are dominant.

Provided the resonance condition may be satisfied, a uniform shear flow which is perturbed by a two-dimensional wave of small but finite amplitude may be unstable, owing to the growth of two initially infinitesimal oblique waves which complete the resonant triad.

$$m\hat{x}_1 = \tfrac{1}{2}kx + ly, \quad m\hat{y}_1 = -lx + \tfrac{1}{2}ky,$$

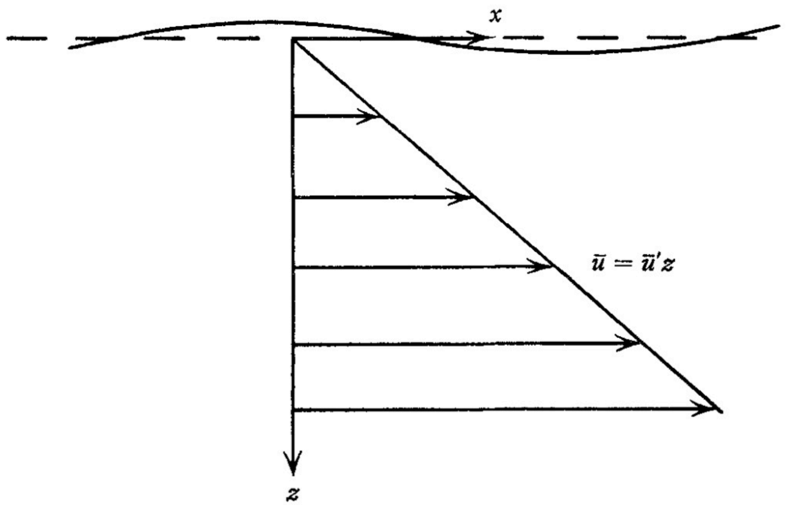

FIGURE 1. The flow configuration.

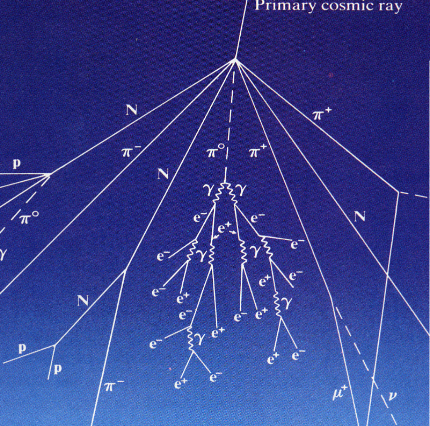

TOROIDAL FLUX TUBE IN A ROTATING STAR

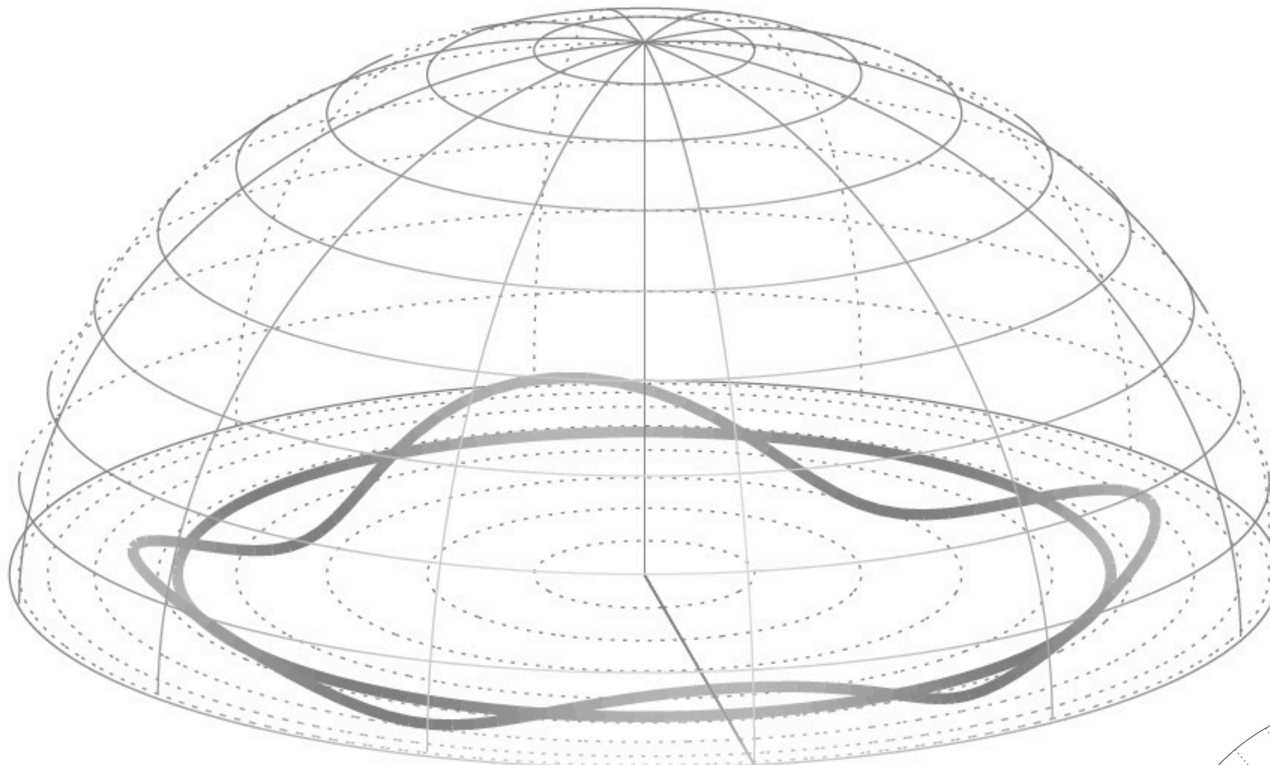

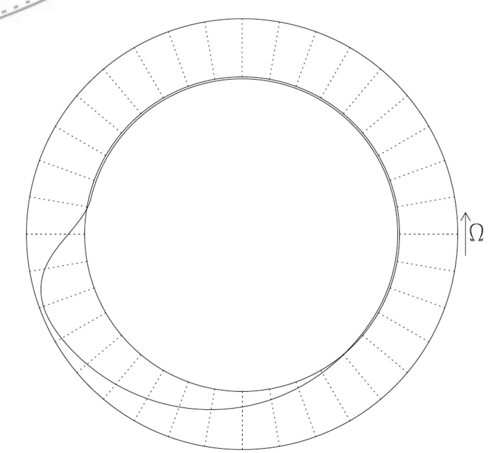

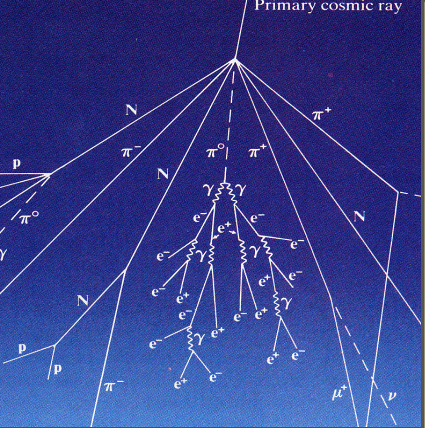

Introduction

Solar activity derived from cosmogenic radionuclides.

Solar activity and the planetary hypothesis

Some basics about solar structure

The Model

Results

6. INDIVIDUAL ASPECTS OF SOLAR/STELLAR ACTIVITY EXPLAINABLE WITH THE FLUX-TUBE APPROACH.

a) Tilt angle of active region's main axis (by typically 10°) with respect to the equator.

Caligari P, Moreno-Insertis F, Schüssler M.: "Emerging flux tubes in the solar convection zone. I: Asymmetry, tilt, and emergence latitude," *ApJ.* **441** 886-902 (1995).

b) Asymmetry between preceding and following part of the active region (as regards morphology, stability, proper motion).

Ferriz-Mas, A. & Schüssler, M.: "On the asymmetry of bipolar active regions," in *Advances in Solar Physics: Three Dimensional Structure of Solar Active Regions*, ASP Conference Series Vol. **155**, pp. 14–18 (1998).

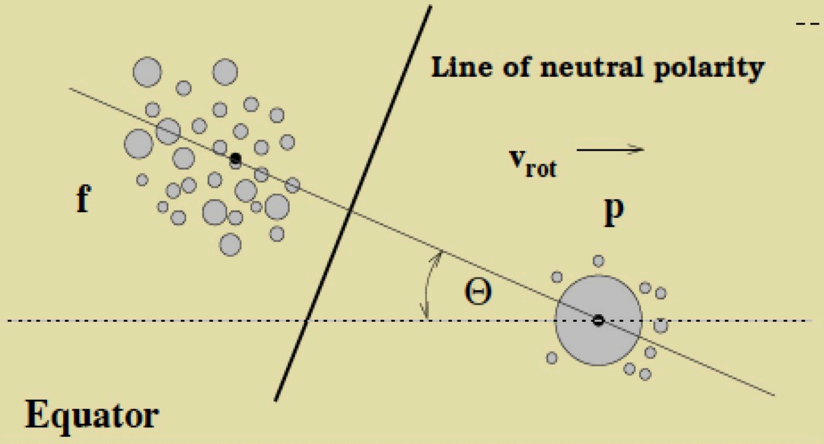

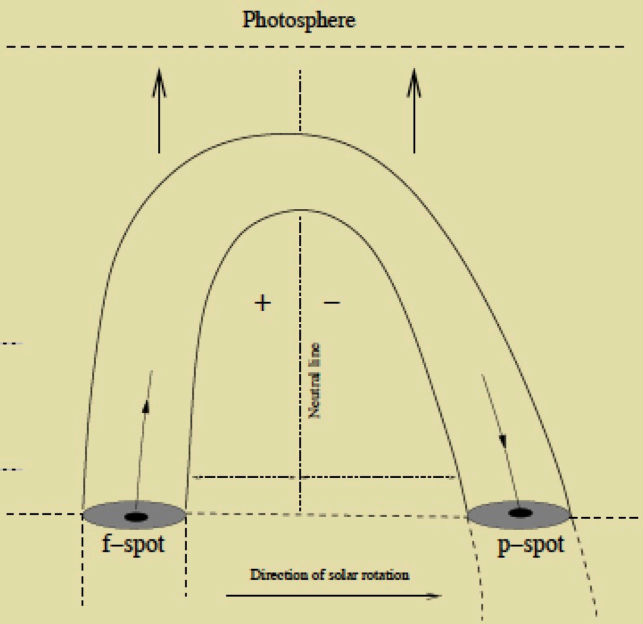

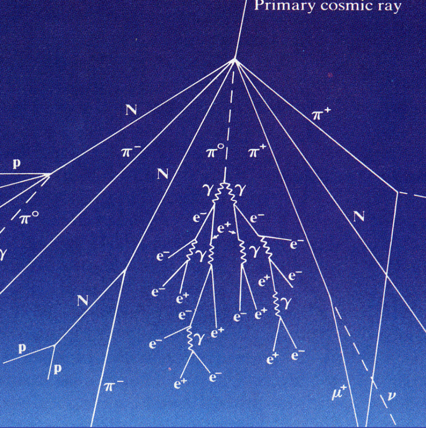

(c) Latitudes of emergence of sunspots.

Schüssler, M., Caligari, P., Ferriz-Mas, A. & Moreno-Insertis, F.: "Instability and eruption of magnetic flux tubes in the solar convection zone," *Astron. Astrophys.* **281**, L69–L72 (1994).

(d) Semi-analytical computation of the (dynamic) α-effect due to instabilities of magnetic flux tubes driven by buoyancy and Coriolis force.

Ferriz Mas, A., Schmitt, D., & Schüssler, M.: "A dynamo effect due to instability of magnetic flux tubes," *Astron. Astrophys.* **289**, 949–956 (1994).

(e) Long intervals ($\simeq 50 - 100$ years) with absence of activity in the form of sunspots (*grand minima* or *Maunder minima*).

Schmitt, D., Schüssler, M. & Ferriz-Mas, A.: "Intermittent solar activity by an on-off dynamo," *Astron. Astrophys.* **311**, L1-L4 (1996).

(f) Possibility of magnetic spots at hight latitudes for T-Tauri stars. Polar spots in rapidly rotating stars.

Schüssler, M., Caligari, P., Ferriz-Mas, A., Solanki, K., & Stix, M.: "Distribution of starspots on cool stars. I. Young and main sequence stars of 1 $M_\odot$," *Astron. Astrophys.* **314**, 503–513 (1996).

Range of application: from T-Tauri stars to red giants.

General reference for the flux-tube approach: Ferriz-Mas, A.: **"Solar interior: convection zone flux tubes,"** in *Encyclopedia of Astronomy and Astrophysics* (2001).

294

A&A 405, 291–301 (2003)
DOI: 10.1051/0004-6361:20030582

Astronomy & Astrophysics

I. Equilibrium and stability properties

V. Holzwarth[1,2] and M. Schüssler[1]

[1] Max-Planck-Institut für Aeronomie, Max-Planck-Str. 2, 37191 Katlenburg-Lindau, Germany
e-mail: schuessler@linmpi.mpg.de
[2] School of Physics and Astronomy, University of St. Andrews, North Haugh, St. Andrews KY16 9SS, UK

Received 28 February 2003 / Accepted 18 April 2003

Abstract. Surface reconstructions of active close binary stars based on photometric and spectroscopic observations reveal non-uniform starspot distributions, which indicate the existence of preferred spot longitudes (with respect to the companion star). We consider the equilibrium and linear stability of toroidal magnetic flux tubes in close binaries to examine whether tidal effects are capable to initiate the formation of rising flux loops at preferred longitudes near the bottom of the stellar convection zone. The tidal force and the deviation of the stellar structure from spherical symmetry are treated in lowest-order perturbation theory assuming synchronised close binaries with orbital periods of a few days. The frequency, growth time, and spatial structure of linear eigenmodes are determined by a stability analysis. We find that, despite their small magnitude, tidal effects can lead to a considerable longitudinal asymmetry in the formation probability of flux loops, since the breaking of the axial symmetry due to the presence of the companion star is reinforced by the sensitive dependence of the stability properties on the stellar stratification and by resonance effects. The orientation of preferred longitudes of loop formation depends on the equilibrium configuration and the wave number of the dominating eigenmode. The change of the growth times of unstable modes with respect to the case of a single star is very small.

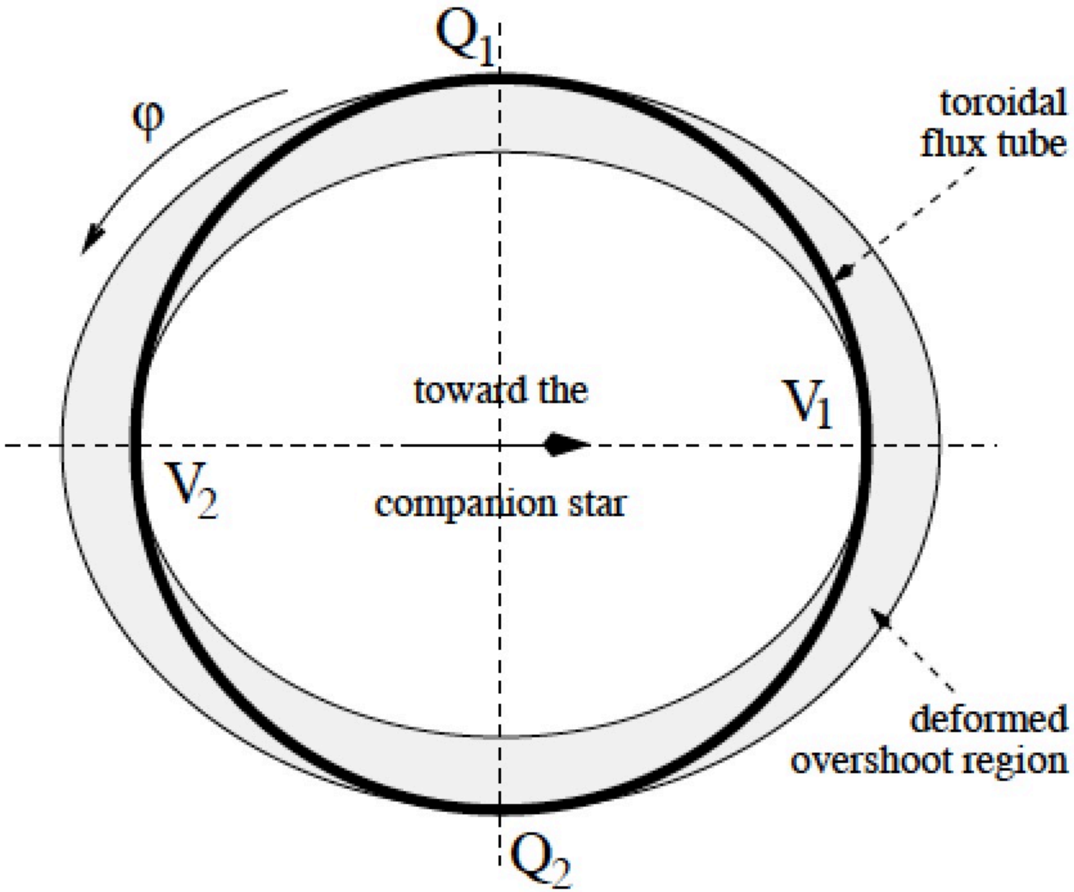

Table 1. Parameters at equilibrium depth r_0 of the reference configuration.

equilibrium depth	$r_0 = 5.07 \times 10^{10}$ cm $= 0.73\,R_\odot$
gas pressure	$p_{e0} = 4.31 \times 10^{13}$ dyn/cm^2
pressure scale height	$H_{p0} = 5.52 \times 10^9$ cm
density	$\rho_{e0} = 0.15$ g/cm^3
density scale height	$H_{\rho 0} = 9.21 \times 10^9$ cm
superadiabaticity	$\delta_0 = -9.77 \times 10^{-7}$
superad. scale height	$H_{\delta 0} = 4.43 \times 10^8$ cm
rotation	$T = 2$ d
binary separation	$a = 8.41\,R_\odot$
expansion parameter	$\epsilon^3 = 6.53 \times 10^{-4}$
deformation parameters	$\bar{r} = 8.16 \times 10^{-4}$
(at equator, $\lambda = 0$)	$\hat{r} = 4.90 \times 10^{-4}$

Dynamic Variations at the Base of the Solar Convection Zone

R. Howe,[1*] J. Christensen-Dalsgaard,[2] F. Hill,[1] R. W. Komm,[1] R. M. Larsen,[3] J. Schou,[3] M. J. Thompson,[4] J. Toomre[5]

We have detected changes in the rotation of the sun near the base of its convective envelope, including a prominent variation with a period of 1.3 years at low latitudes. Such helioseismic probing of the deep solar interior has been enabled by nearly continuous observation of its oscillation modes with two complementary experiments. Inversion of the global-mode frequency splittings reveals that the largest temporal changes in the angular velocity Ω are of the order of 6 nanohertz and occur above and below the tachocline that separates the sun's differentially rotating convection zone (outer 30% by radius) from the nearly uniformly rotating deeper radiative interior beneath. Such changes are most pronounced near the equator and at high latitudes and are a substantial fraction of the average 30-nanohertz difference in Ω with radius across the tachocline at the equator. The results indicate variations of rotation close to the presumed site of the solar dynamo, which may generate the 22-year cycles of magnetic activity.

The differential rotation of the sun and its ability to generate large-scale magnetic fields through cyclic dynamo action appear to be intimately linked. It is thought that the global dynamo behavior (*1*) responsible for the emergence of large active regions (sunspot groups) is derived from strong organized toroidal magnetic fields generated by rotational shear in a thin region, called the tachocline, at the base of the convection zone. The evolving magnetic field could well have a feedback effect on the fluid

reduced at a period of 1.0 year compared with 1.3 years (the power is lower at a period of 1.0 year by a factor of 4), so it is improbable that the variations detected at the equator are a product of systematic annual changes in observing conditions or of the orbit of SOHO. Furthermore, although the variations illustrated in Fig. 4 do have a dominant period of 1.0 year, the signal at this period is apparent only near $0.72R$ and 60° (Fig. 4, C and D), which again argues against the variations being caused by annual systematic observational errors.

The results of the analysis of one million random time series are summarized in table 2. The second column shows how many of the simulated time series had lines falling into the defined windows. The third column shows the corresponding probability. The 4th column lists the number of coincidences with the previous lines (1-2, 1-3, 1-4, 1-5). Although in none of our simulations all 5 lines occurred simultaneously, the probability of such a case can be calculated from the third column.

Period window	Counts	Probability	Coincidence	Coincidence probability
85-89	63381	0.063		Observed / calculated
103-106	47484	0.047	2583	0.0026 / 0.0030
146-151	85557	0.086	167	0.00017 / 0.00025
206-210	110761	0.111	13	$1.3\ 10^{-5}$ / $2.8\ 10^{-5}$
503-515	1044	0.0011	0	--- / $3.0\ 10^{-8}$

Table 2. Results of the Monte Carlo runs simulating random time series.

The probability that all 5 lines occur simultaneously is $3.1\ 10^{-8}$ which, as expected, never occurred during the 1,000,000 test runs.

Wavelet analysis corresponding to planetary torque for the case 1.
Periodicities centered at 88, 208 and 500 years.
Note however that the amplitudes are is very small.

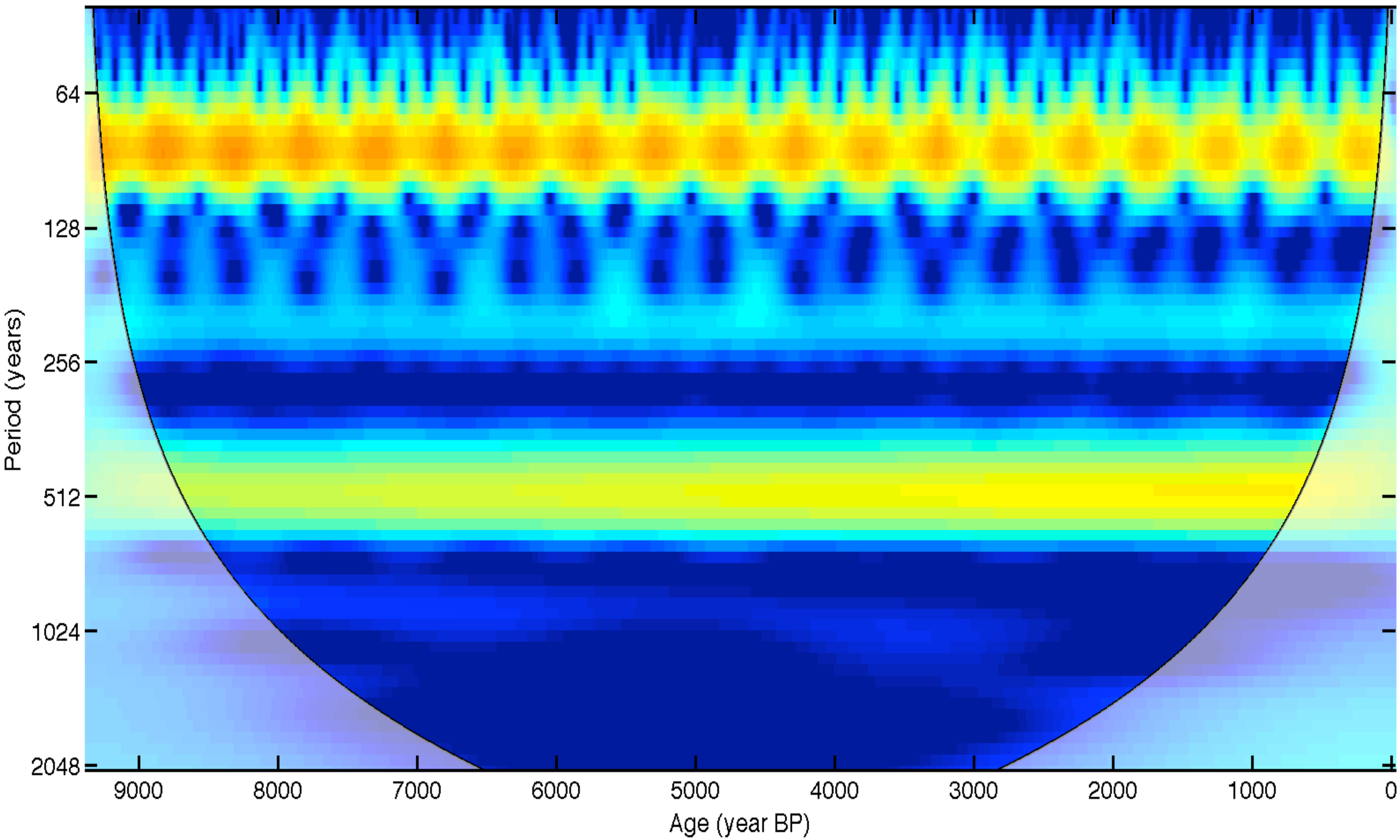

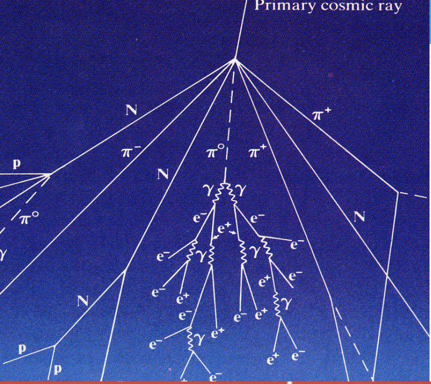

The planetary hypothesis

- Jose's results points to Spin-Orbit coupling
- Tidal acceleration is the only coupling interaction
- Proportional to M/d^3

	Distance (AU)	Mass (M_E)	Period (yr)	Displacement of Sun (Md)	Gravitational Force (M/d^2)	Tide (M/d^3)
Mercury	0.31-0.47	0.055	0.24	0.02	0.25-0.57	**0.53-1.85**
Venus	0.72	0.815	0.62	0.59	1.57	**2.18**
Earth	1	1	1	1	1	**1**
Mars	1.52	0.107	1.88	0.16	0.05	0.03
Jupiter	5.2	318	11.86	**1654**	11.76	**2.26**
Saturn	9.54	95	29.46	**906**	1.04	0.11
Uranus	19.18	15	84.01	**288**	0.04	0.002
Neptune	30.06	17	164.8	**511**	0.02	0.0006

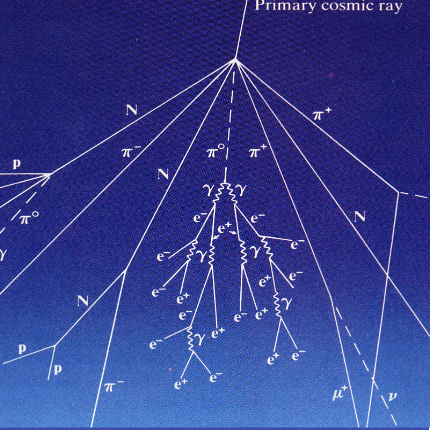
Primary cosmic ray

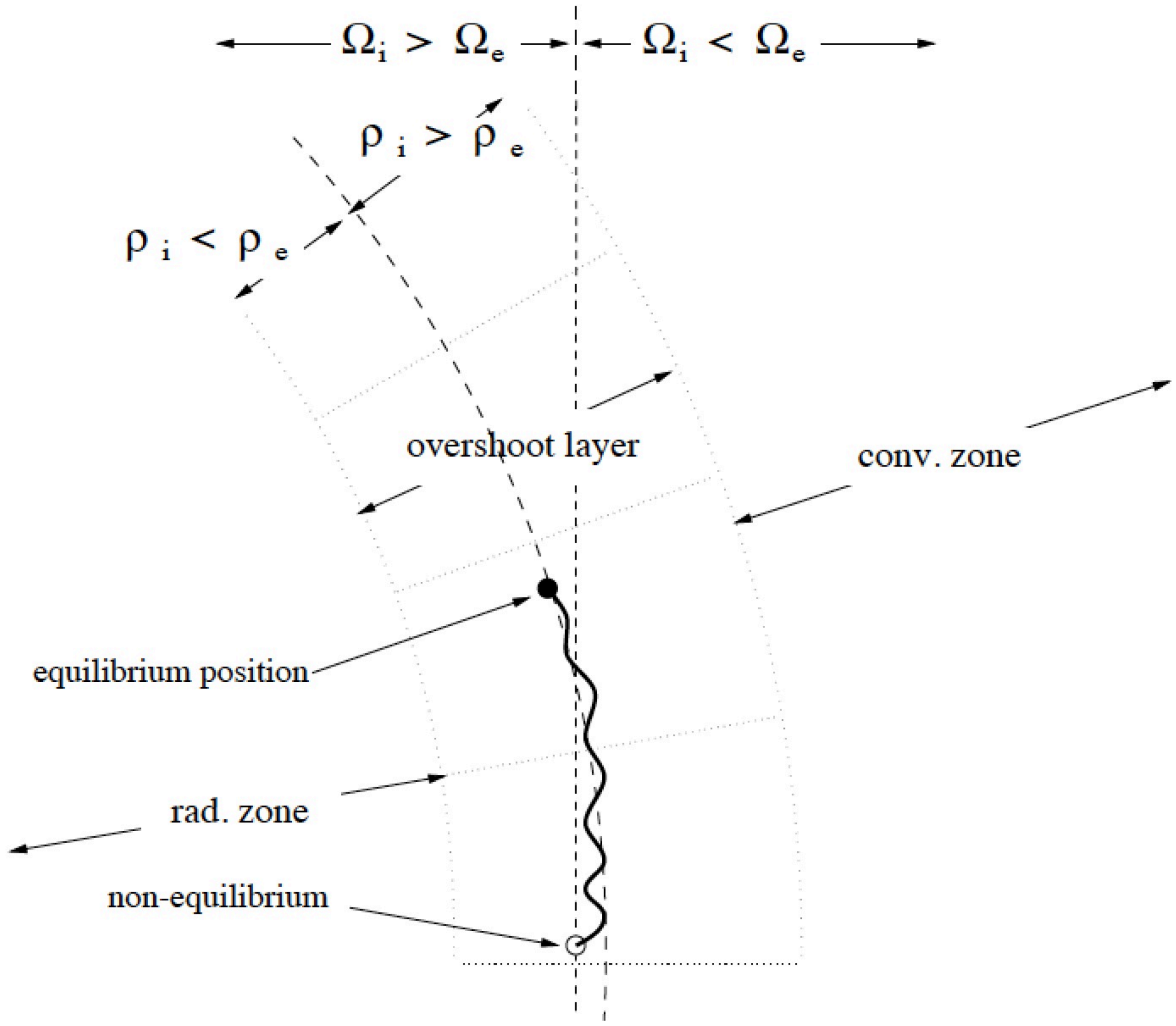
$\Omega_i > \Omega_e$
$\Omega_i < \Omega_e$
$\rho_i > \rho_e$
$\rho_i < \rho_e$
overshoot layer
conv. zone
equilibrium position
rad. zone
non-equilibrium

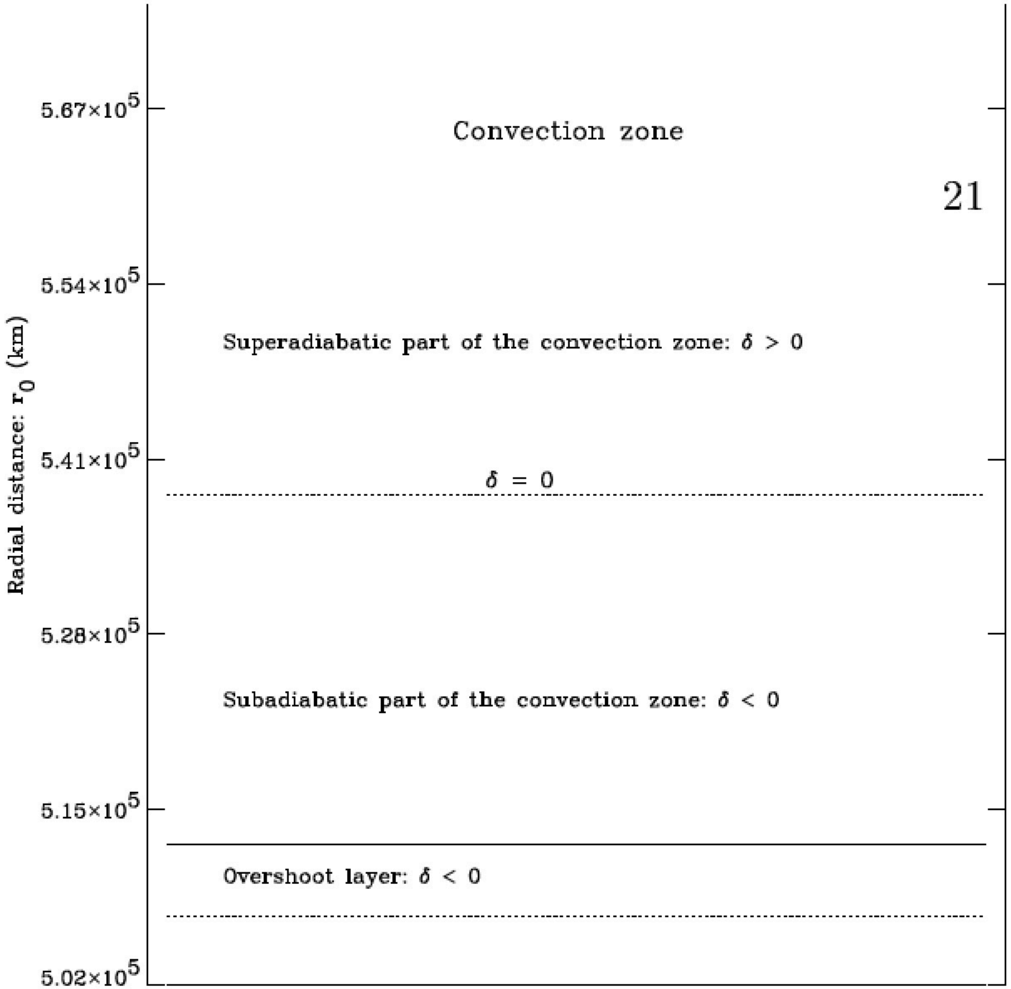

Beginning of the radiative zone

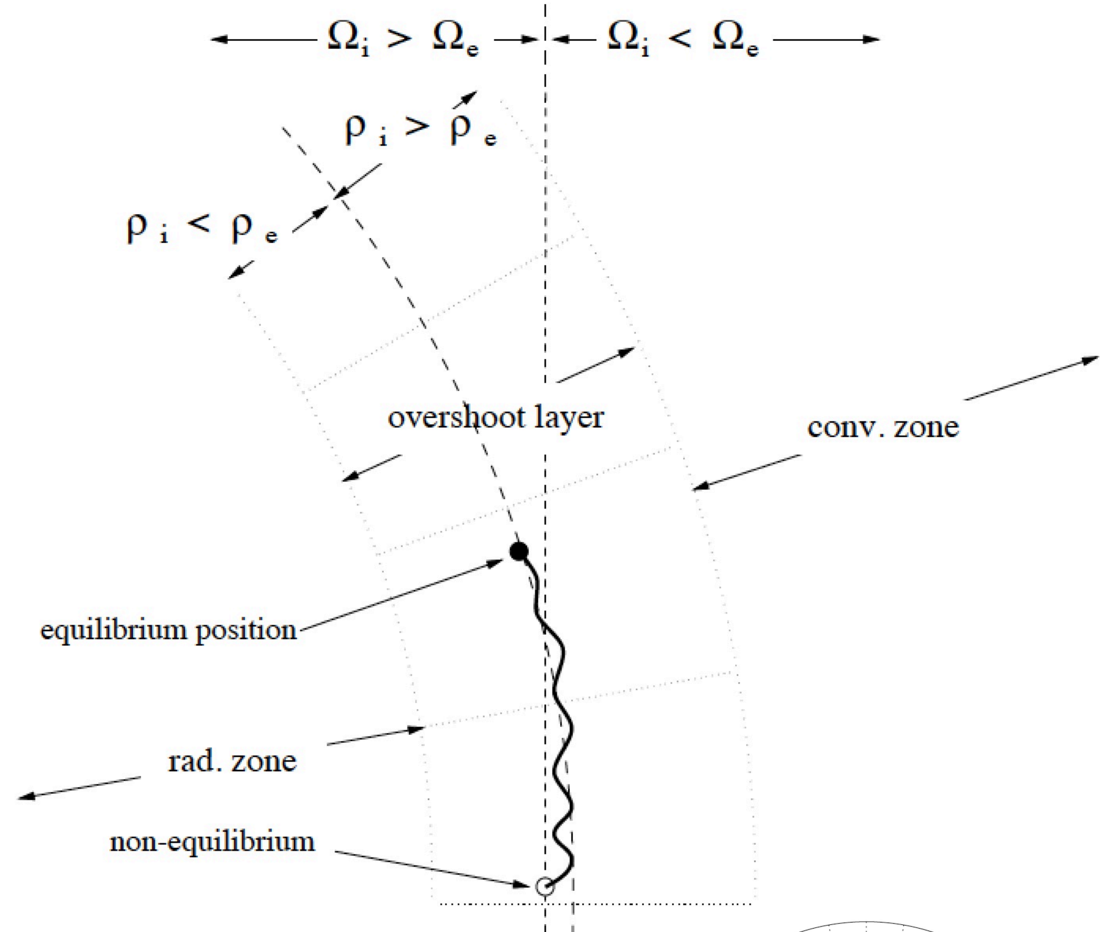

TOROIDAL FLUX TUBE IN A ROTATING STAR

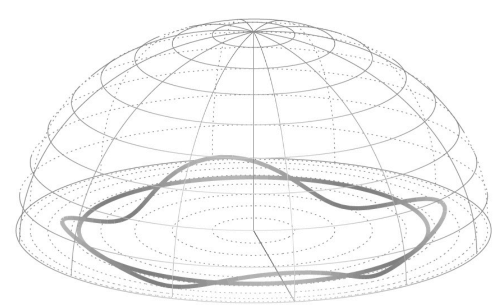

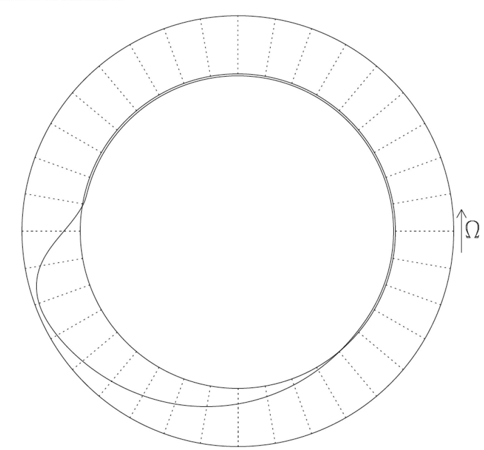

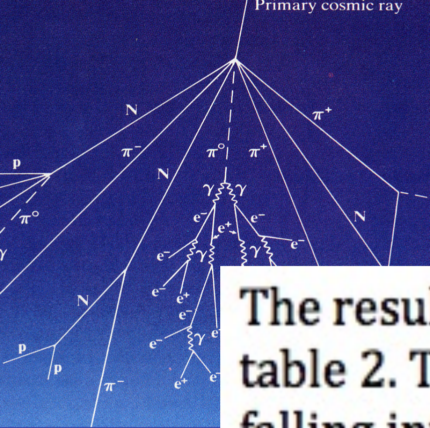

The next point we address now is the question whether the good agreement between 10Be and 14C with the torque can occur just by chance. We use a random generator and produce artificial time series of the same length (7000 years). Then we calculate the Fourier spectrum, select the periods between 40 and 1200 years and test whether one or several of the 20 strongest lines fall within one or several windows defined for the 5 selected spectral lines in table 1.

The results of the analysis of one million random time series are summarized in table 2. The second column shows how many of the simulated time series had lines falling into the defined windows. The third column shows the corresponding probability. The 4th column lists the number of coincidences with the previous lines (1-2, 1-3, 1-4, 1-5). Although in none of our simulations all 5 lines occurred simultaneously, the probability of such a case can be calculated from the third column.

Period window	Counts	Probability	Coincidence	Coincidence probability
85-89	63381	0.063		Observed / calculated
103-106	47484	0.047	2583	0.0026 / 0.0030
146-151	85557	0.086	167	0.00017 / 0.00025
206-210	110761	0.111	13	$1.3\ 10^{-5}$ / $2.8\ 10^{-5}$
503-515	1044	0.0011	0	--- / $3.0\ 10^{-8}$

Table 2. Results of the Monte Carlo runs simulating random time series.

The probability that all 5 lines occur simultaneously is $3.1\ 10^{-8}$ which, as expected, never occurred during the 1,000,000 test runs.

SECULAR INCREASE OF ASTRONOMICAL UNIT FROM ANALYSIS OF THE MAJOR PLANET MOTIONS, AND ITS INTERPRETATION

G.A. KRASINSKY and V.A. BRUMBERG

Institute of Applied Astronomy, Russain Academy of Sciences, Kutuzov Quay 10, 191187 St. Petersburg, Russia, e-mail: kra@quasar.ipa.nw.ru

(Received: 26 April 2004; revised: 4 June 2004; accepted: 9 June 2004)

Abstract. From the analysis of all available radiometric measurements of distances between the Earth and the major planets (including observations of martian landers and orbiters over 1971–2003 with the errors of few meters) the positive secular trend in the Astronomical Unit AU is estimated as $\frac{d}{dt}\mathrm{AU} = 15 \pm 4\,\mathrm{m/cy}$. The given uncertainty is the 10 times enlarged formal error of the least-squares estimate and so accounts for possible systematic errors of measurements and deficiencies of the mathematical model. The reliability of this estimate as well as its physical meaning are discussed. A priori most plausible attribution of this effect to the cosmological expansion of the Universe turns out inadequate. A model of the observables developed in the frame of the relativistic background metric of the uniform isotropic Universe shows that the corresponding dynamical perturbations in the major planet motions are completely canceled out by the Einstein effect of dependence of the rate of the observer's clock (that keeps the proper time) on the gravitational field, though separately values of these two effects are quite large and attainable with the accuracy achieved. Another tentative source of the secular rate of AU is the loss of the solar mass due to the solar wind and electromagnetic radiation but it amounts in $\frac{d}{dt}\mathrm{AU}$ only to $0.3\,\mathrm{m/cy}$. Excluding other explanations that seem exotic (such as secular decrease of the gravitational constant) at present there is no satisfactory explanation of the detected secular increase of AU, at least in the frame of the considered uniform models of the Universe.

Key words: cosmology, ephemerides, relativity, astronomical unit

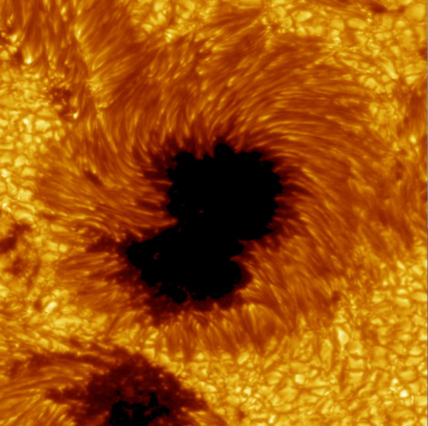

Kernreaktionen

$$^{14}N + n \Rightarrow {}^{10}Be + 3p + 2n$$

$$^{14}N + p \Rightarrow {}^{10}Be + 4p + 1n$$

$$^{16}O + n \Rightarrow {}^{10}Be + 4p + 3n$$

$$^{16}O + p \Rightarrow {}^{10}Be + 5p + 2n$$

$$^{14}N + n \Rightarrow {}^{14}C + p$$

GRIP Eisbohrkern

Eine 55 cm Probe Eis $\approx$ 900 g

1 Atome Be $\rightarrow$ 10^{18} Moleküle

Carrier ^{9}Be pro Probe $\approx$ 0.3 mg

Typische Verhältnisse $^{10}Be/^{9}Be \approx 10^{-12} - 10^{-14}$ (Messung)

D.h.

In 900 g $\rightarrow$ $^{10}Be \approx 10^{4}$ Atome pro Probe

Beispiel aus ^{14}C

$$^{14}C/^{12}C(t = 1950) \approx 10^{-12}$$

$$1 \text{ gr Kohle} \approx 6\ 10^{10}\ {}^{14}C \text{ Atome}$$

$$r_{c14} = \frac{14}{60\,s} \approx 0.2 \text{ counts pro Sekunde. 48 Stunden um } 0.5\%$$

$$r_{bms} \approx 100 \text{ counts pro Sekunde. 10 Minuten um } 0.5\%$$

dafür reicht mg Material

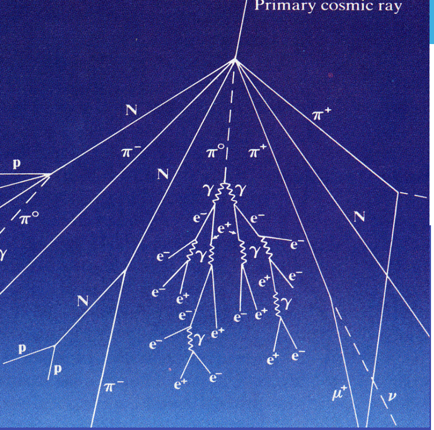

Transport of cosmic rays in the Heliosphere (Parker, 1965)

$$\frac{\partial f}{\partial t} = -(\mathbf{V} \cdot \nabla) f - \mathrm{div}\,(\hat{\kappa}\,\mathbf{grad}\; f) + \frac{1}{3}\,\mathrm{div}\,\mathbf{V}\,\frac{\partial f}{\partial \ln p} + Q\,,$$

f : cosmic ray distribution function

p : particle momentum

V : solar wind speed

$\hat{k}$: diffusion tensor

Q : local production

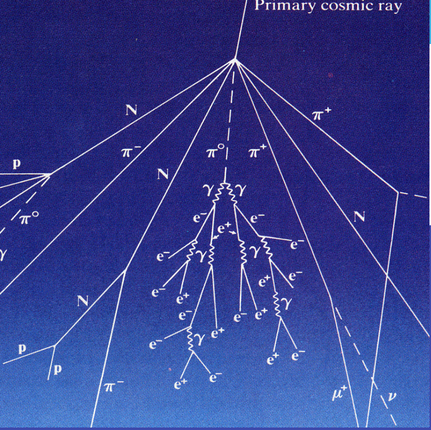

Force Field Approximation (Gleeson and Axford, 1968)

(1) Q=0

(2) Steady state: $\frac{\partial f}{\partial t} = 0$

(3) Adiabatic energy loss rate: $\frac{pV}{3f} \, grad\, f = 0$

- Spherical symmetry: $\hat{k} = k\hat{I}$

- $k = k_1(r)P, \quad (P \equiv \frac{pc}{q} \text{ rigidity})$

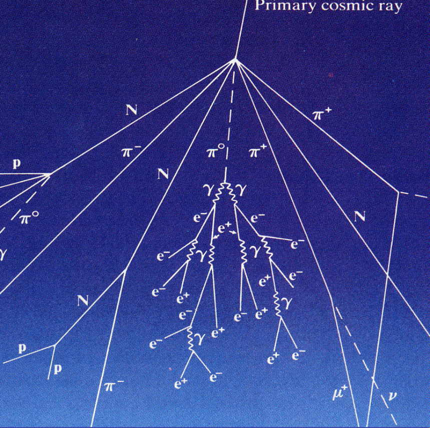

^{10}Be as function of ϕ

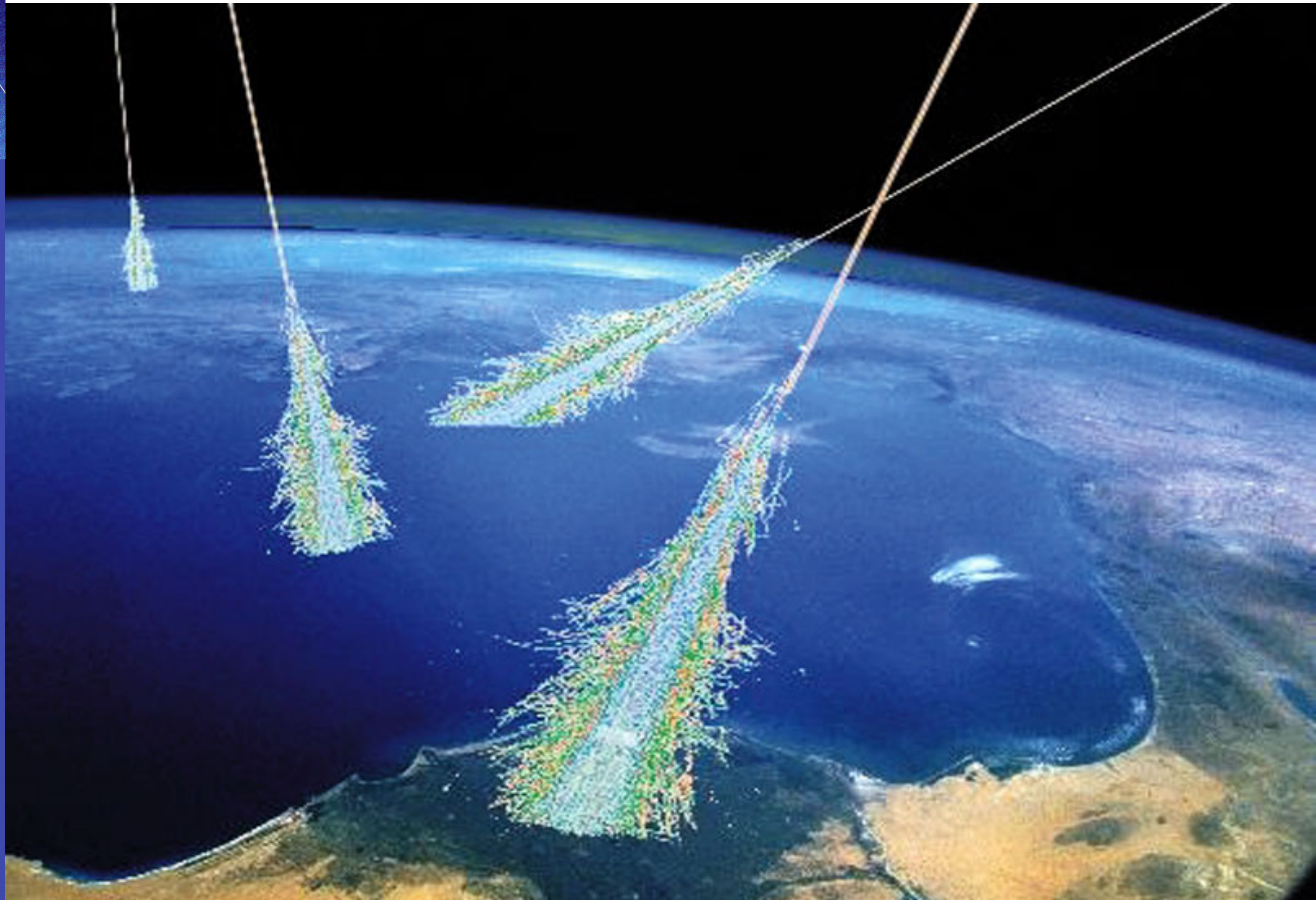

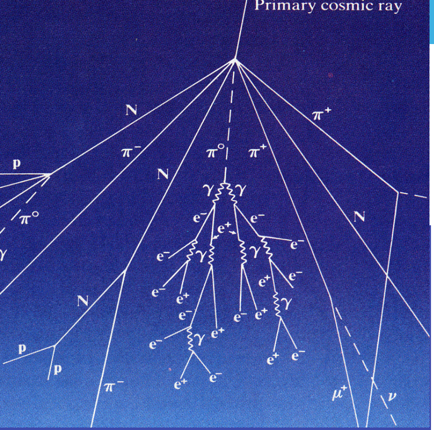

^{10}Be as function of ϕ

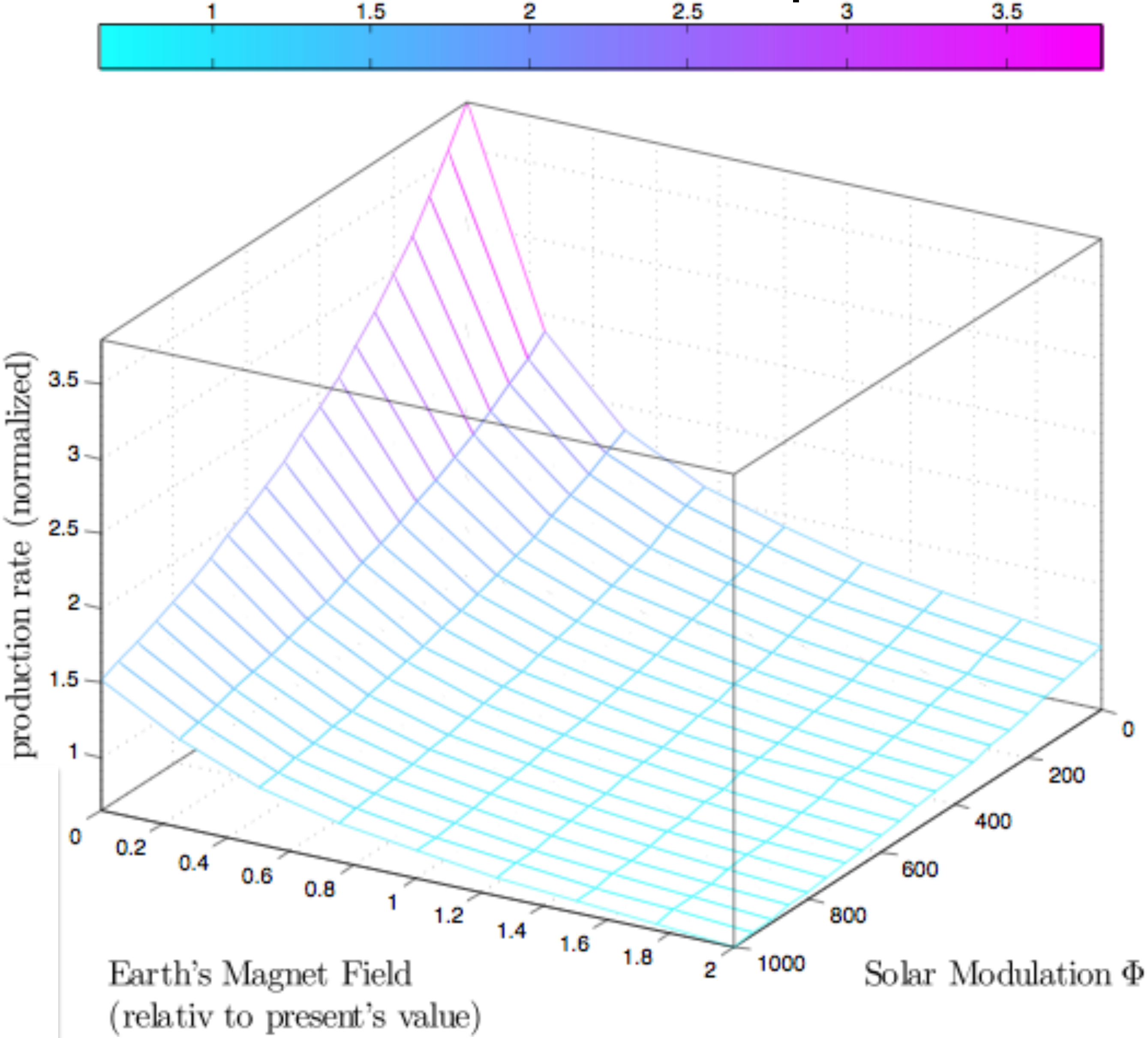

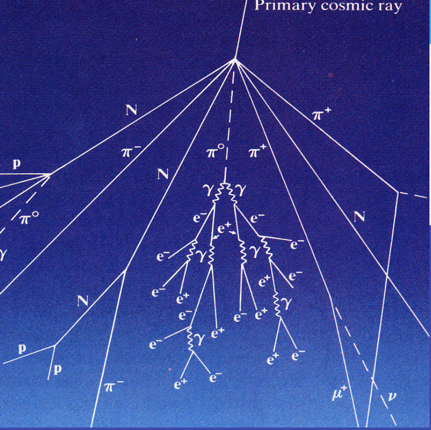

Transport of cosmic rays in the Heliosphere

$$\frac{\partial f}{\partial t} + \frac{V}{3k_1}\frac{\partial f}{\partial P} = 0$$

f : cosmic ray distribution function
P: particle momentum
V: solar wind
k_1: diffusion

- Formally equal to collisionless Boltzmann eq.

with an electric field: $E(r) \equiv \frac{V(r)}{3k_1(r)}$

- Electric potential: $\phi(r) \equiv \int_r^{r_b} E(x) = \int_r^{r_b} \frac{V(x)}{3k_1(x)}$

The effect of solar wind on cosmic rays can be described by an electric potential!

=> ϕ parameterize the level of solar activity

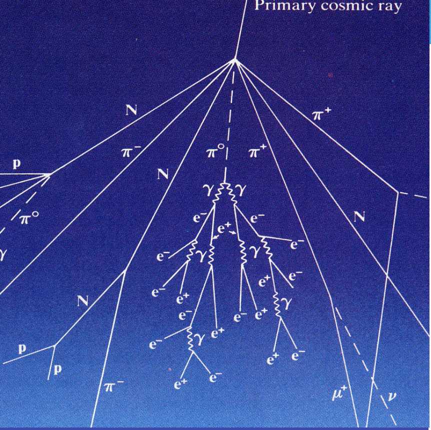

Significance of the spectral agreement

We address now i the question whether the good agreement between ^{10}Be and ^{14}C with the torque can occur by chance.

- We use a random generator and produce artificial time series of the same length (1,000,000 test runs)
- We calculate the Fourier spectrum, select the periods between 40 and 1200 y and test whether one or several of the 20 strongest lines fall within the windows defined for 5 selected spectral lines in table 1.

Table 1: Coincidence of spectral lines in several records.

Period window	^{10}Be concentr.	^{14}C production	ϕ	Torque
85-89	86	88	88	86
103-106	104	105	105	104
146-151	148	150	150	147
206-210	207	209	209	209
503-515	504	512	508	504

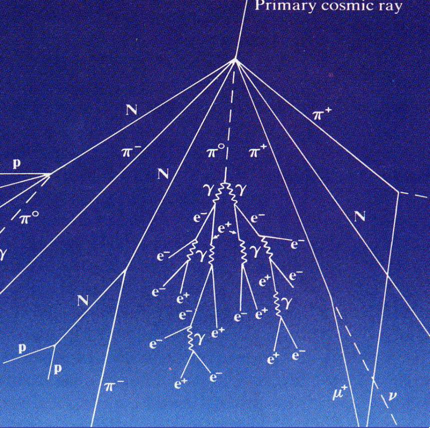

Significance of the spectral agreement

We address now the question whether the good agreement between ^{10}Be and ^{14}C with the torque can occur by chance.

- We use a random generator and produce artificial time series of the same length (1,000,000 test runs)
- We calculate the Fourier spectrum, select the periods between 40 and 1200 y and test whether one or several of the 20 strongest lines fall within the windows defined for 5 selected spectral lines in table 1.

Table 2: Results of the Monte Carlo runs simulating random time series of ϕ with a white spectrum.

Period window	Counts	Probability	Coincidence	Coincidence probability
85-89	143095	0.143		Observed / calculated
103-106	103835	0.104	13697	0.0137 / 0.0149
146-151	168087	0.168	1886	0.0019 / 0.0025
206-210	189785	0.189	261	$2.61\ 10^{-4}$ / 4.7410^{-4}
503-515	1064	0.0011	0	0 / 5.0410^{-7}

Is there a planetary influence on solar activity?

Jose A. Abreu; J. Beer, A. Ferriz-Mas, K. G. McCracken & F. Steinhilber

Abreu et al. (2012)
Astronomy & Astrophysics

EGU Congress Vienna | Austria | 07 – 12 April 2013

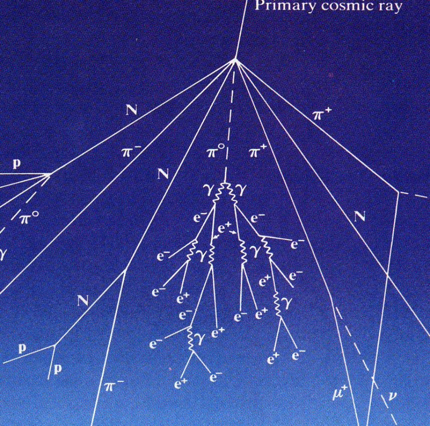

- ❑ The solar activity parameterized by the so-called **solar modulation potential** ϕ **=>** solar activity = **solar modulation potential** ϕ
- ❑ Cosmogenic radionuclides as function of ϕ & geomagnetic field

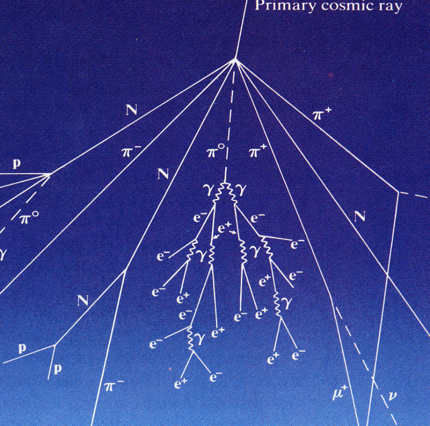

Introduction

Solar activity derived from cosmogenic radionuclides.

Solar activity and the planetary hypothesis

Some basics about solar structure

The Model

Results

Conclusions

Talk Summary:

Planetary influence on solar activity evidenced by cosmogenic radionulclides

- ❑ Solar activity derived from cosmogenic radionuclides
- ❑ Solar activity and the planetary hypothesis.
- ❑ Some basics about solar structure
- ❑ The model
- ❑ Results
- ❑ Conclusions

Abreu et al. (2012)
Astronomy & Astrophysics

Solar motion around barycenter

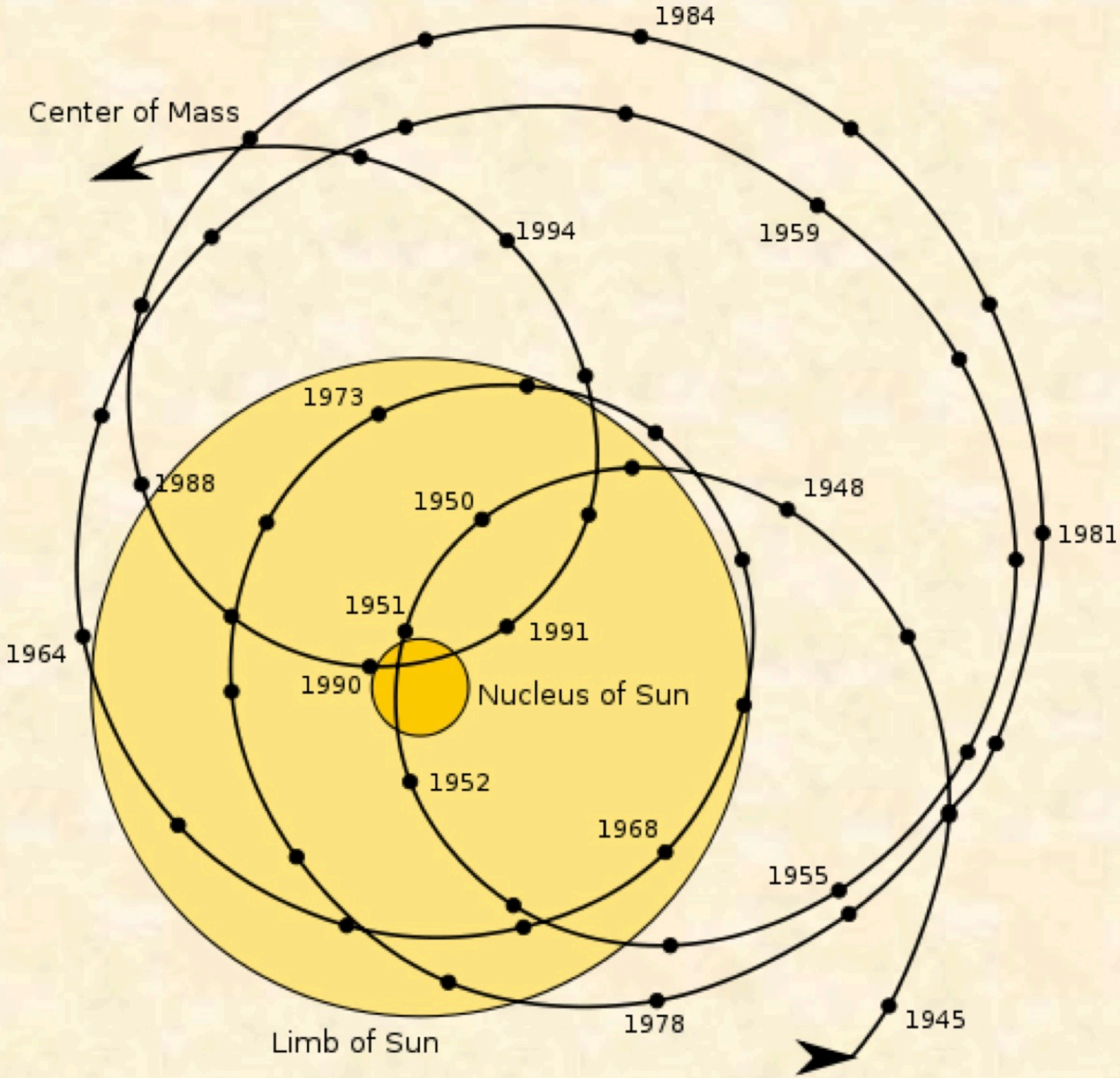

-tween solar activity (sunspots,

g(1967), Blizard(1969), Wood

A reports.

Jose (1965)

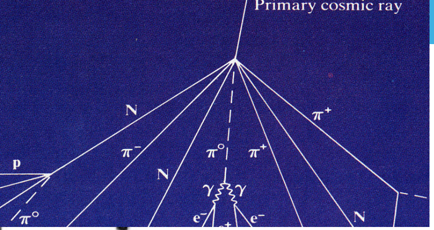

The planetary hypothesis Jose (1965)

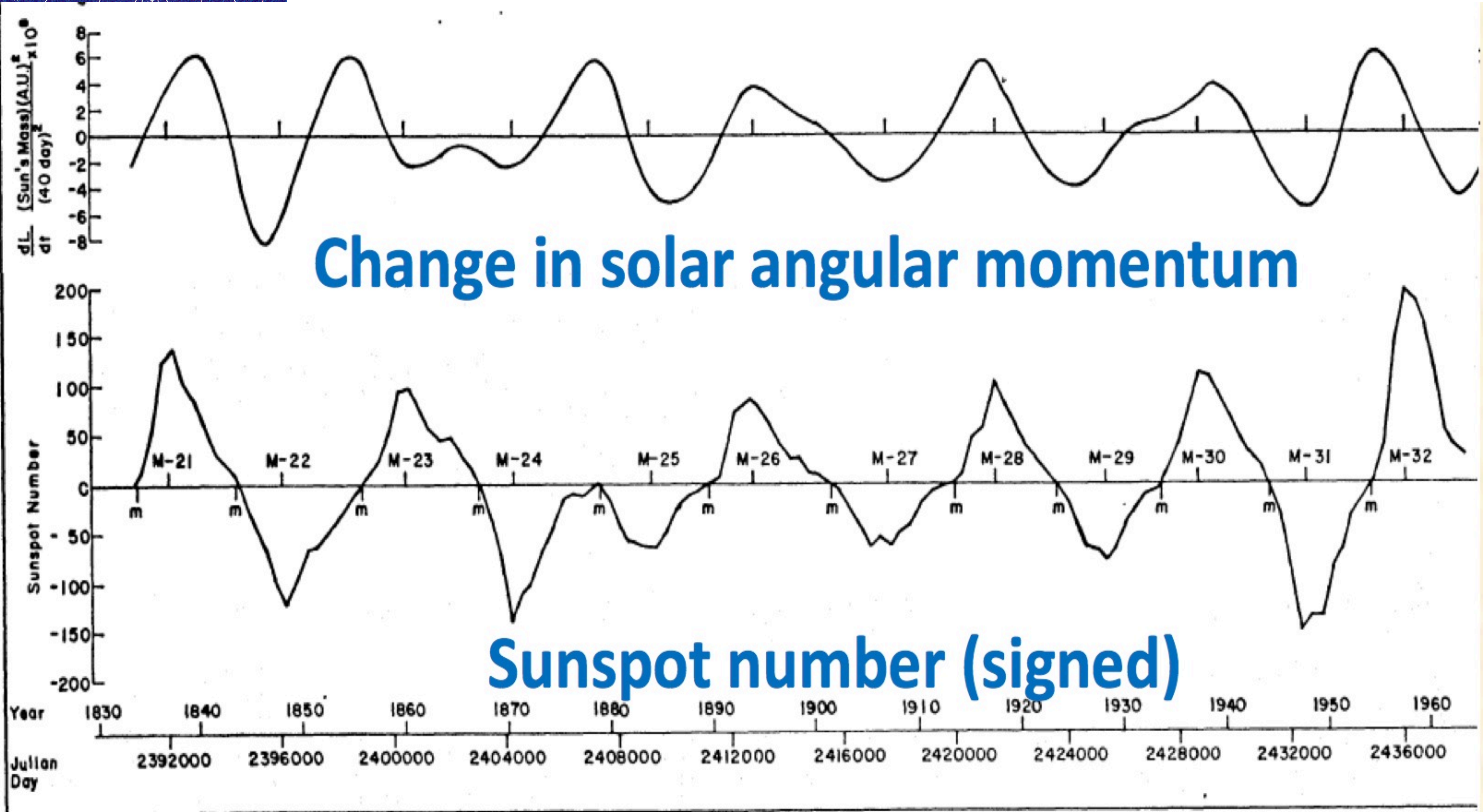

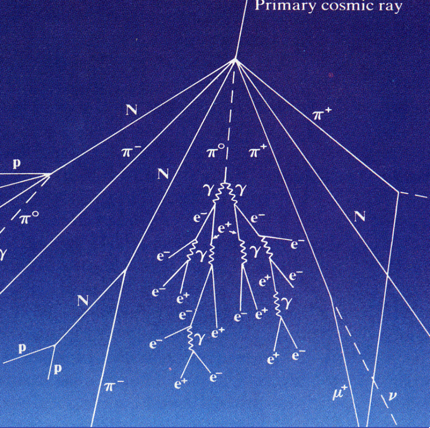

The planetary hypothesis

- Jose's results points to Spin-Orbit coupling
- Tidal acceleration is the only physically relevant interaction
- Proportional to M/d^3.
- The planetary Tides on the Sun are ~ 10^{-12} surface gravity

  (for comparison on the Earth g_{moon}/g_{earth} ~ 10^{-7})
- Tide height (equilibrium tide) on the Sun does not exceed 1 mm!
- Mean daily work of tides is ~10^{28} J (Trellis, 1966)
- Comparable to energy release of the most important flares ~10^{26} J
- Comparable to the magnetic energy of the solar cycle:

$$\frac{d\phi}{dt} = 5\,10^{13}\ \mathrm{Wb/day}$$ (Galloway & Weiss 1981)

$$E_{mag} = \frac{R}{\mu}\,\phi\,B$$ (Ferriz-Mas & Steiner 2007)

For a field at the base of convection zone 1 T and 10 T => E_{mag}~10^{28} J and 10^{29} J

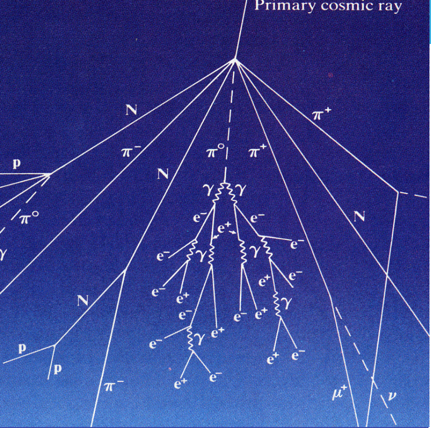

Introduction

Solar activity derived from cosmogenic radionuclides.

Solar activity and the planetary hypothesis

Some basics about solar structure

The Model

Results

Conclusions

Solar activity & the planetary hypothesis

- Wolf (1848) devised a way of quantifying sunspot activity, the Wolf sunspot number and calculated a period for the cycle of 11.1 years

He noted the coincidence with Jupiter's orbital period of 11.8 years

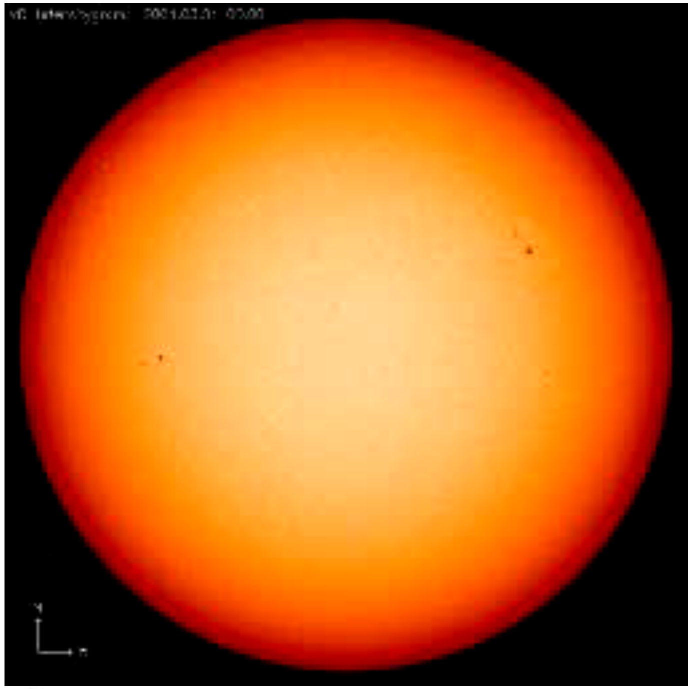

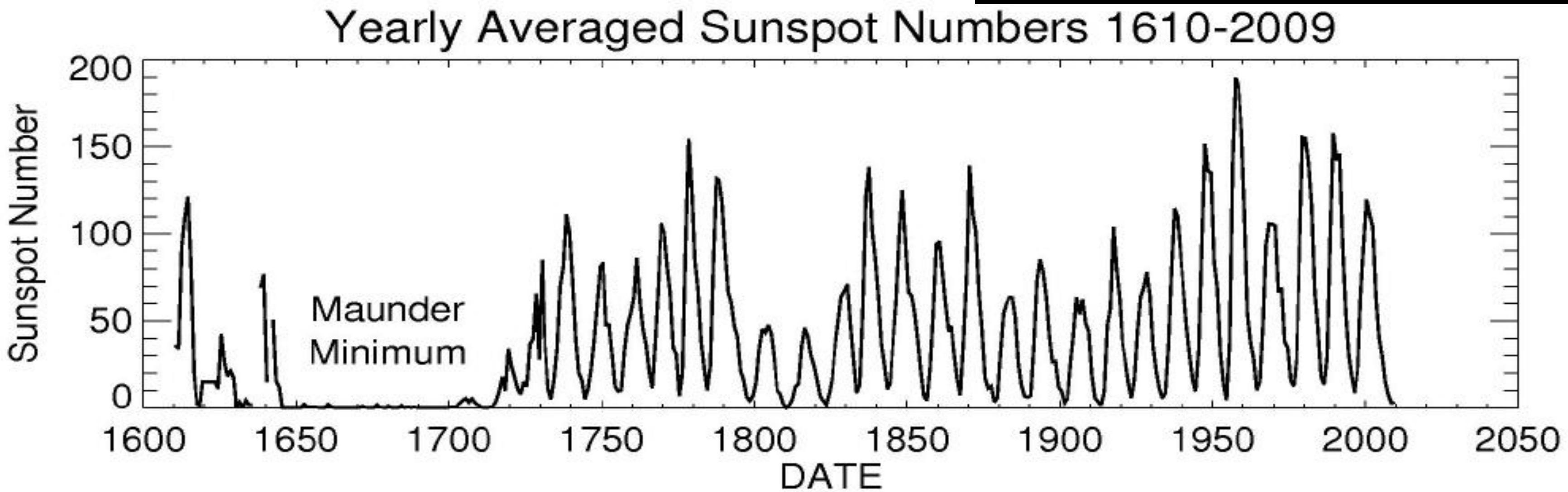

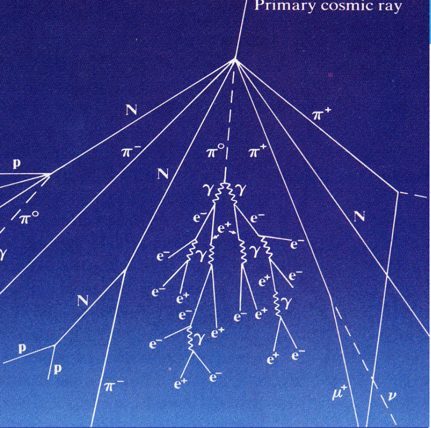

Introduction

Solar activity derived from cosmogenic radionuclides.

Solar activity and the planetary hypothesis

Some basics about solar structure

The Model

Results

Conclusions

Solar activity & the planetary hypothesis

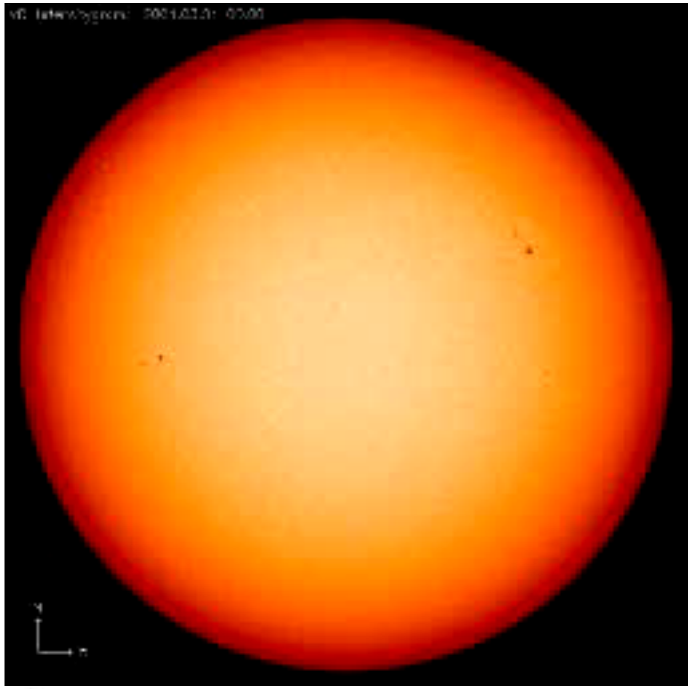

- Schwabe (1843) suggested the existence of an 11 y cycle in sunspots.
- Wolf (1848) devised a way of quantifying sunspot activity, the Wolf sunspot number and calculated a period for the cycle of 11.1 years
  He noted the coincidence with Jupiter's orbital period of 11.8 years

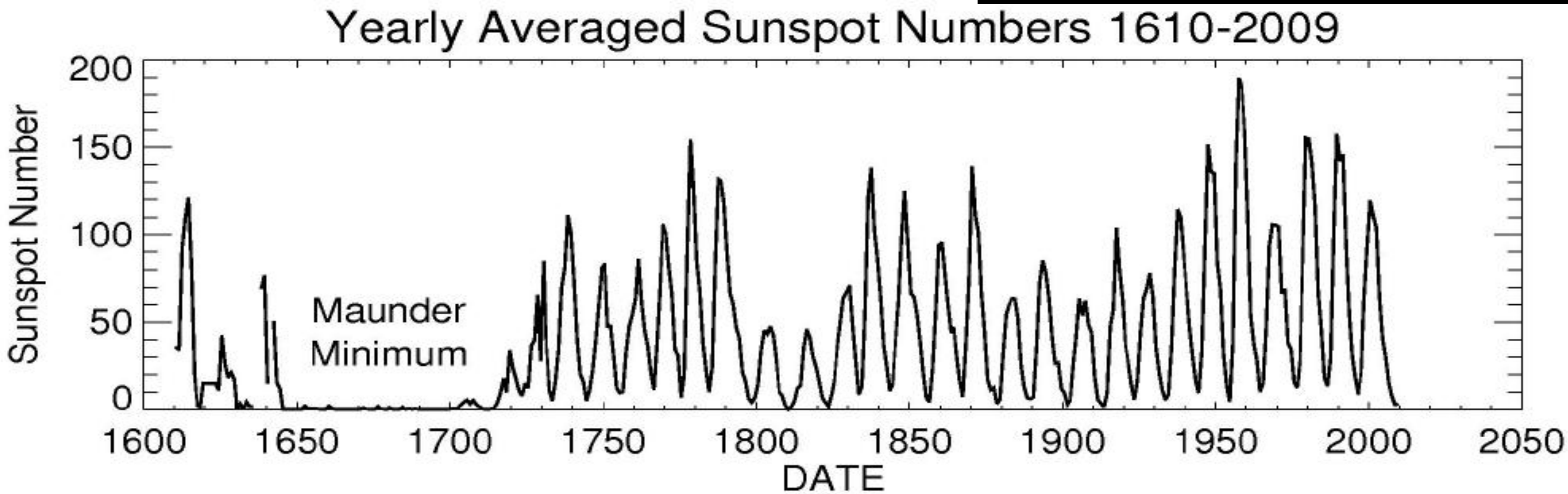

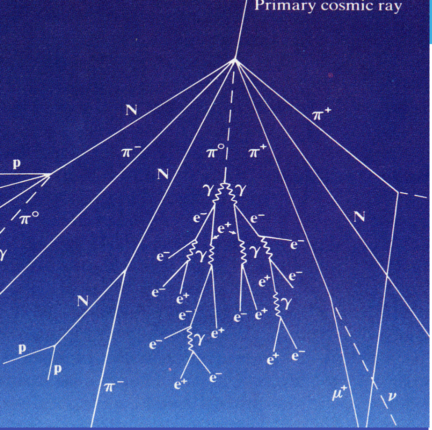

The planetary hypothesis

- Previous estimations show that the planets cannot be the cause of the 11 years solar cycle. (this would produce large changes in the orbital parameters....)
- ...however it could perturb the action of the solar dynamo.
- Planetary hypothesis usually rejected on the basis that tidal accelerations are too weak

But:

- Neglects possible resonance between natural oscillation of the solar interior and tides which may amplify the tidal deformation (Cowling, 1941).

Lunar tide 10^{-7} g_{Earth} => ~ 50 cm

Milankovitch theory of glaciations: small forcing => large climate changes.

- Neglects the possibility that some internal layers –relevant for dynamo action– may already be distorted => torques

At the interface between the convection zone and the radiative interior there is a thin shear layer known as tachocline. Which is inferred to depart significantly from the spherical symmetry (Charbonneau et al., 1999)

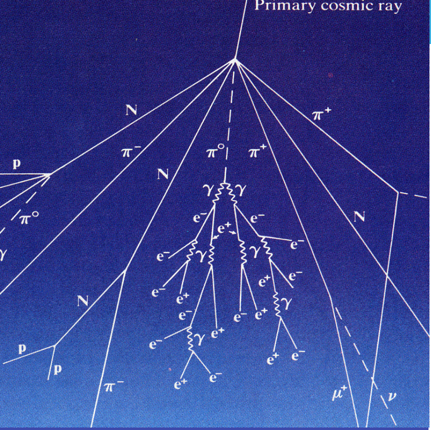
Primary cosmic ray

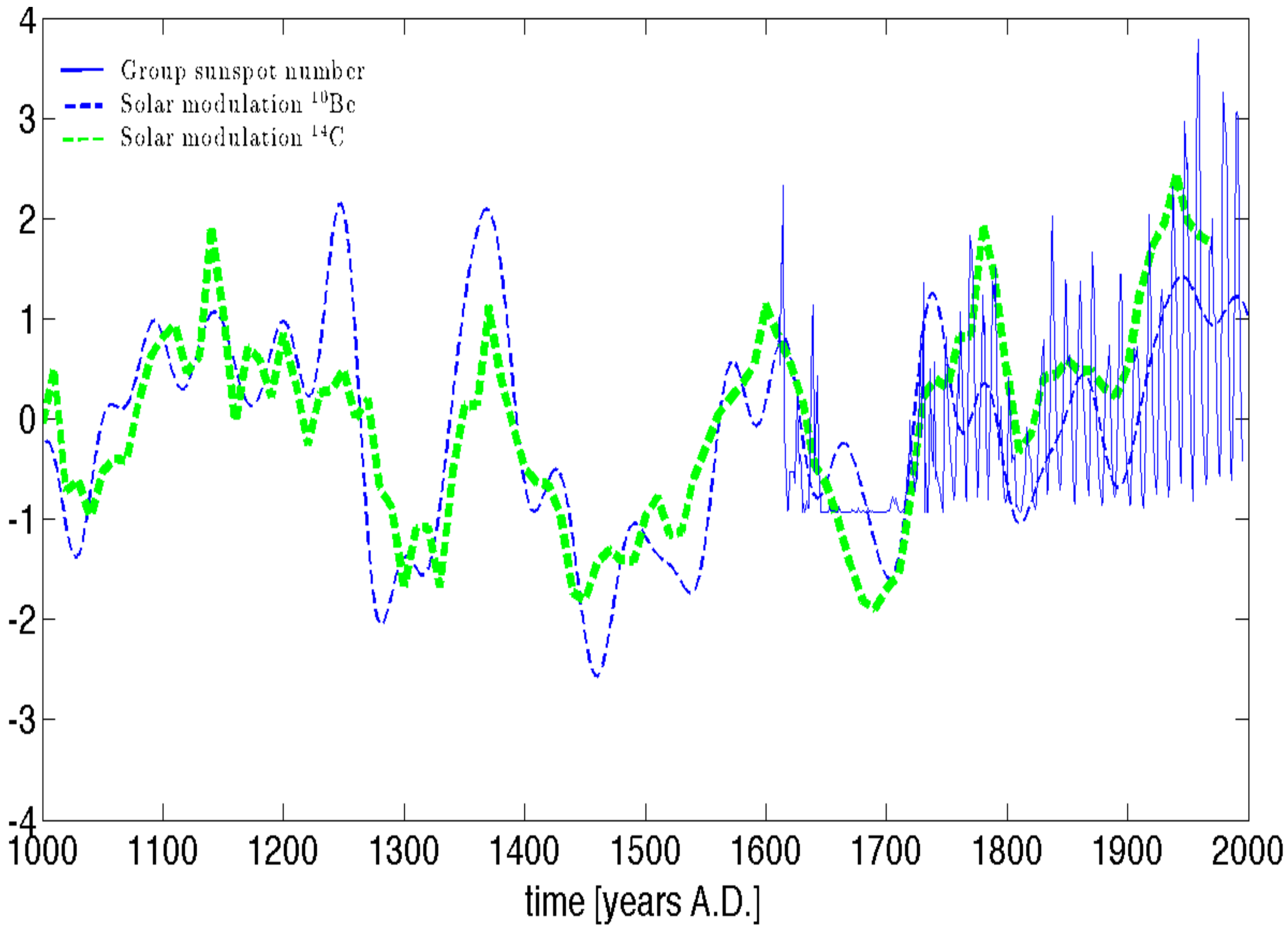

Group sunspot number
Solar modulation ¹⁰Be
Solar modulation ¹⁴C
4
3
2
1
0
-1
-2
-3
-4
1000
1100
1200
1300
1400
1500
1600
1700
1800
1900
2000
time [years A.D.]

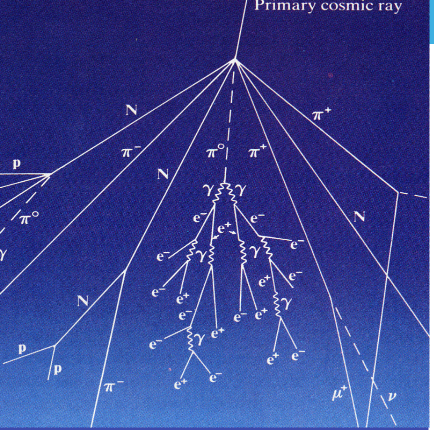

What can cosmogenic radionulides tell us about the possible link?

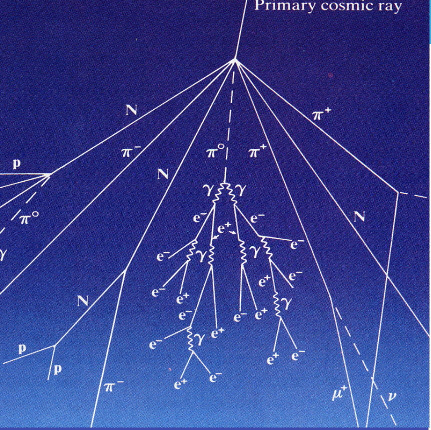

Solar activity and ϕ

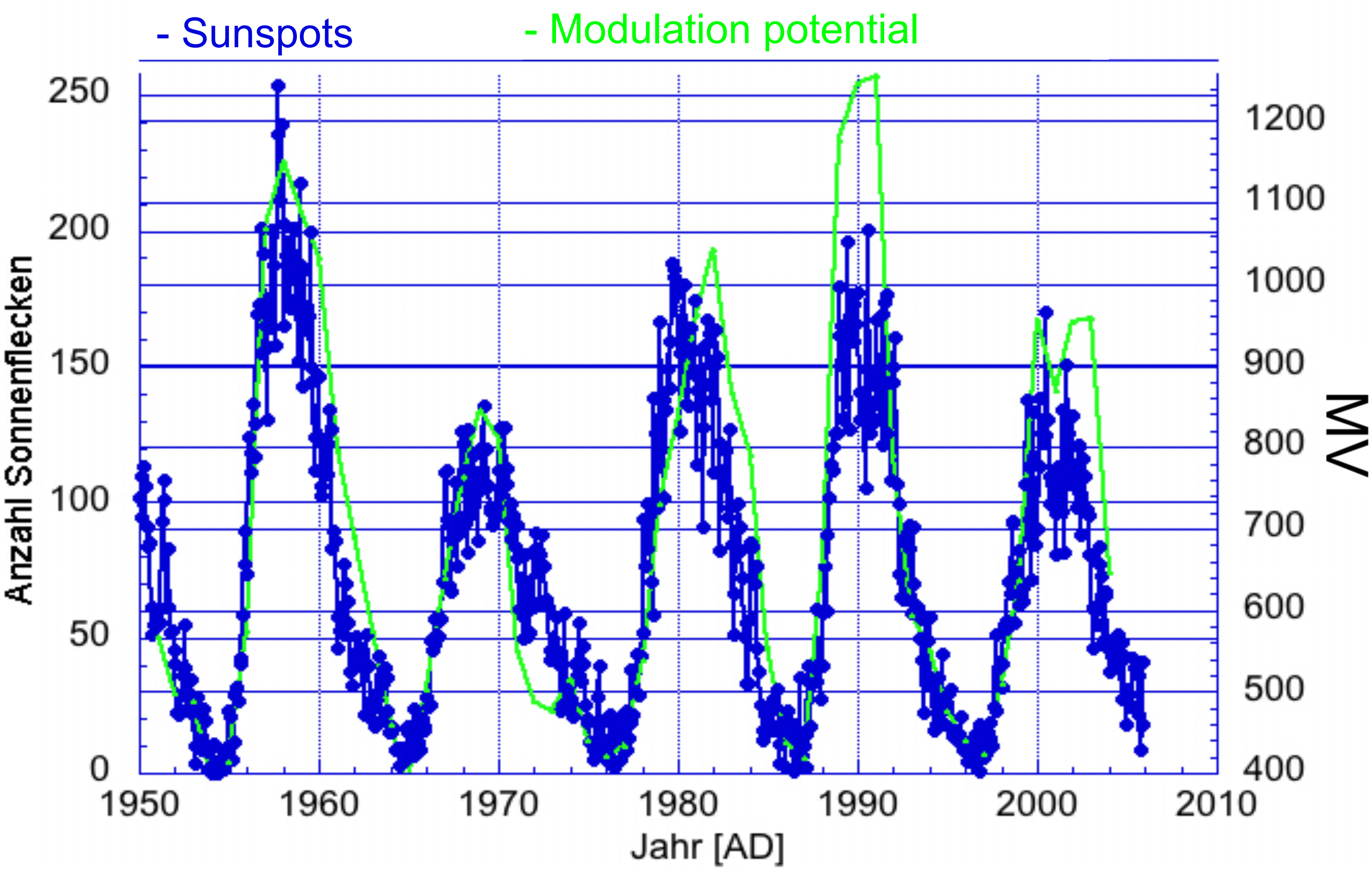

a) Solar activity for the last 10,000 years, Φ determined using ^{10}Be and ^{14}C
b) Wavelet analysis. Red high power.

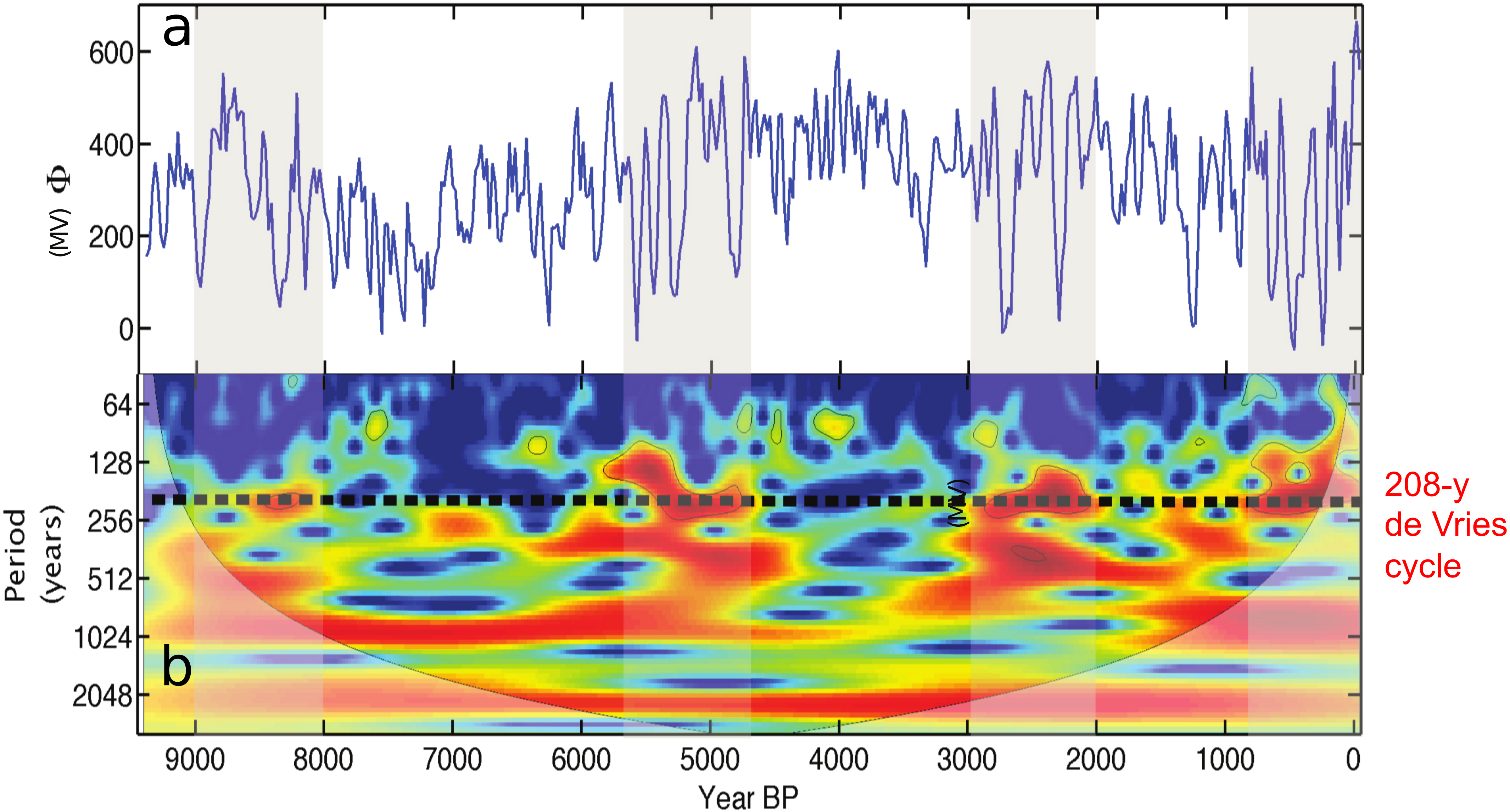

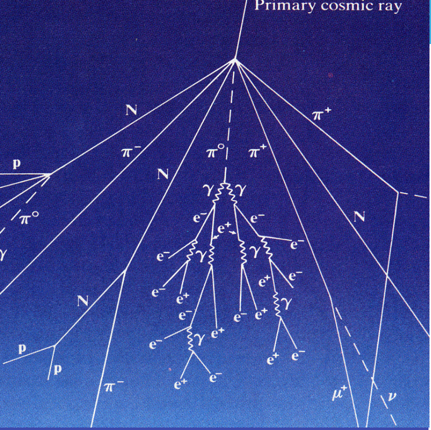

The tachocline and the overshoot layer

- The tachocline may play a fundamental role in the generation and storage of the toroidal magnetic flux that eventually gives rise to solar active regions
- The relative position between these two boundary layers –one mechanical and one thermal– determines the degree of subadiabaticity of the tachocline and therefore its capability to store magnetic flux tubes
- The base of the convection zone, as determined from helioseismology, shows no perceptible deviation from sphericity. The tachocline, however, is inferred to depart significantly from the spherical symmetry
- Charbonneau et al. (1999) inferred a prolate geometry, with an ellipticity a factor 10^3 larger than the solar ellipticity at photospheric level (which is 4 times larger than the Earth's ellipticity.)

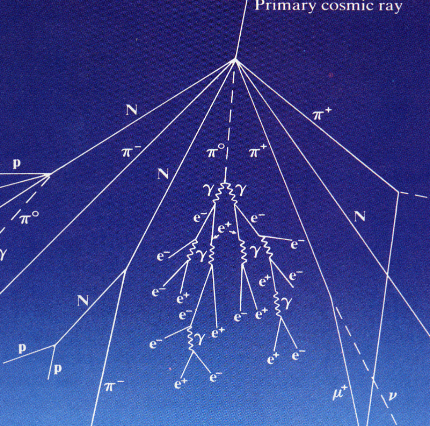

Introduction

Solar activity derived from cosmogenic radionuclides.

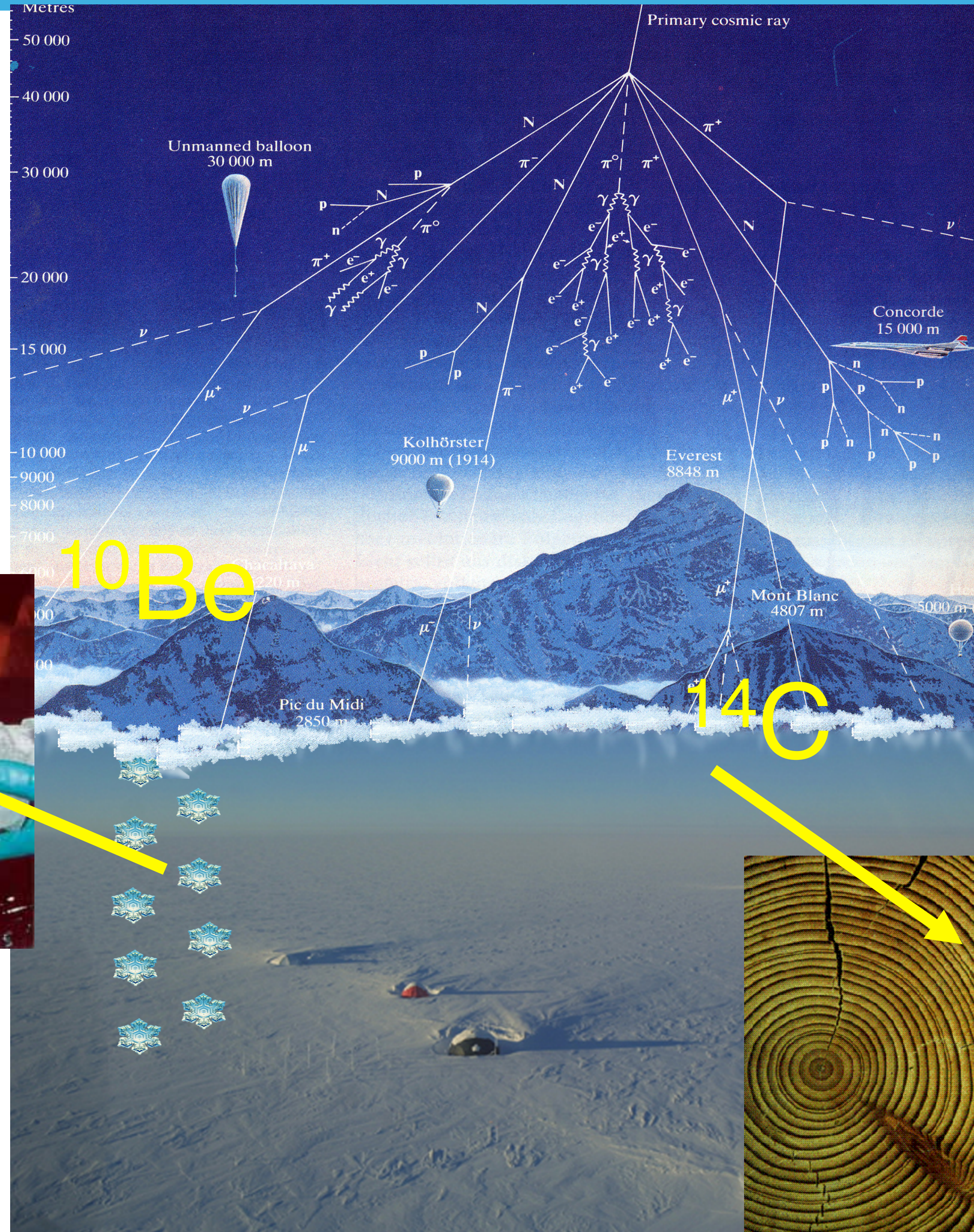

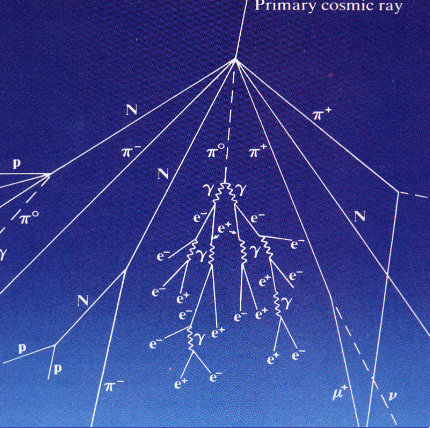

The tachocline and the overshoot layer

- The tachocline may play a fundamental role in the generation and storage of the toroidal magnetic flux that eventually gives rise to solar active regions
- The relative position between these two boundary layers –one mechanical and one thermal– determines the degree of subadiabaticity of the tachocline and therefore its capability to store magnetic flux tubes
- The base of the convection zone, as determined from helioseismology, shows no perceptible deviation from sphericity. The tachocline, however, is inferred to depart significantly from the spherical symmetry
- Charbonneau et al. (1999) inferred a prolate geometry, with an ellipticity a factor 10^3 larger than the solar ellipticity at photospheric level (which is 4 times larger than the Earth's ellipticity.)

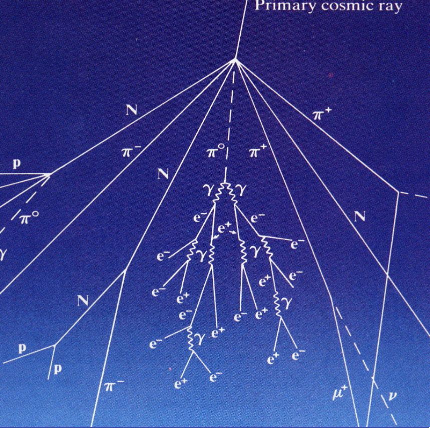

Introduction

Solar activity derived from cosmogenic radionuclides.

Solar activity and the planetary hypothesis

Some basics about solar structure

The Model

Results

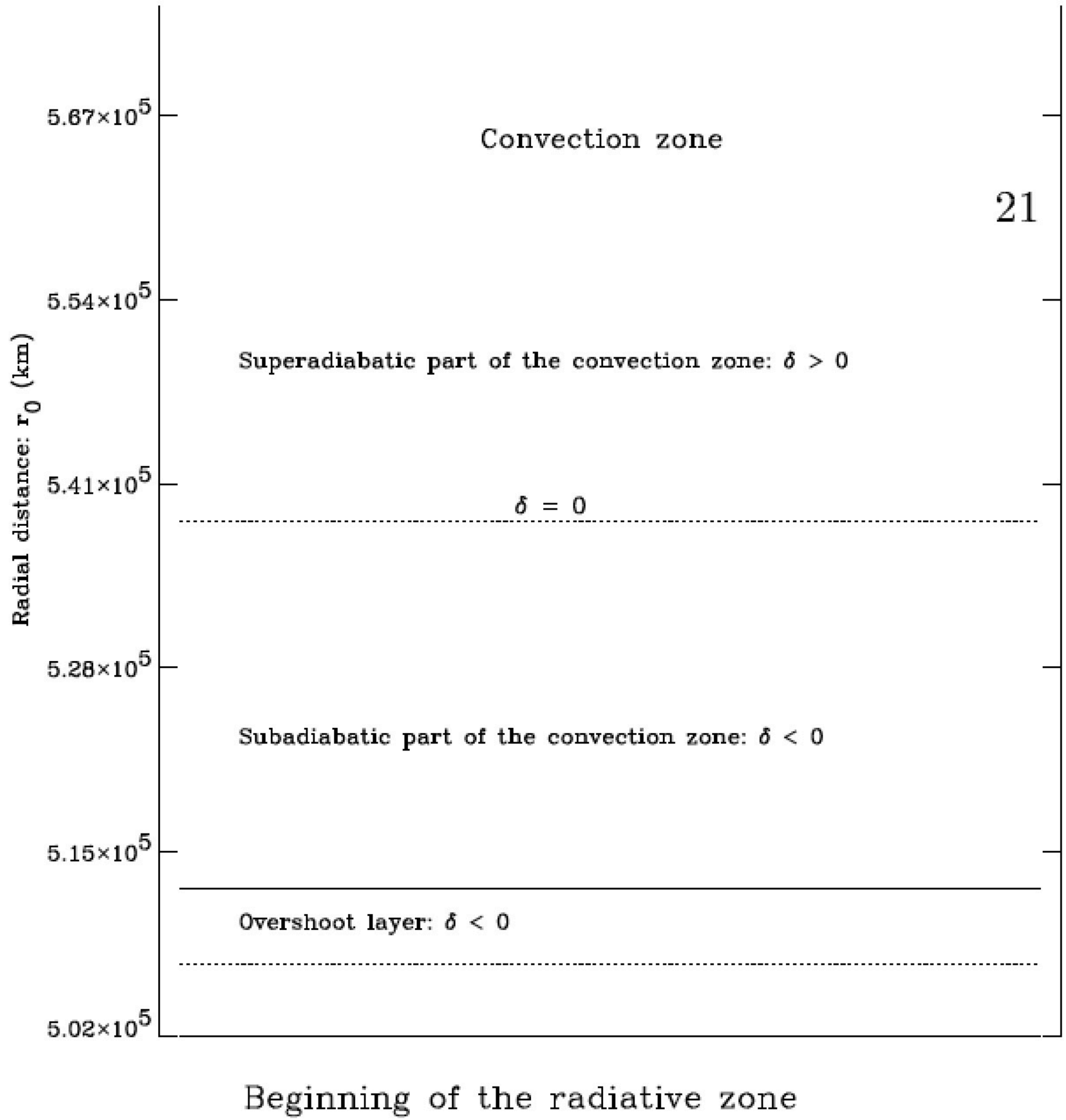

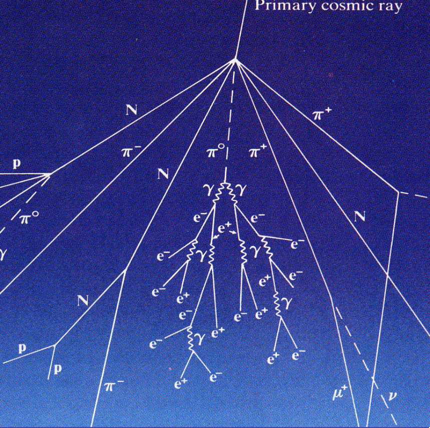

Introduction

Solar activity derived from cosmogenic radionuclides.

Solar activity and the planetary hypothesis

Some basics about solar structure

The Model

Results